USP7 is essential for maintaining Rad18 stability and DNA damage tolerance

Zlatanou, Anastasia; Stewart, Grant; Agathanggelou, Angelo; Stankovic, Tatjana; Miller, Edward

DOI:
10.1038/onc.2015.149

USP7 is essential for maintaining Rad18 stability and DNA damage tolerance

Zlatanou A[1], Sabbioneda S[2], Miller ES[1], Greenwalt A[3], Aggathanggelou A[1], Maurice MM[4], Lehmann AR[5], Stankovic T[1], Reverdy C[6], Colland F[6], Vaziri C[3] , Stewart GS[1]*

[1]School of Cancer Sciences, University of Birmingham, Vincent Drive, Edgbaston, Birmingham, B15 2TT, UK. [2]Istituto di Genetica Molecolare, Consiglio Nazionale delle Ricerche, 27100 Pavia, Italy. [3]Department of Pathology and Laboratory Medicine, University of North Carolina, Chapel Hill, Chapel Hill, NC 27599, USA. [4]University Medical Center, Utrecht (UMCU), Heidelberglaan 100, 3584CX Utrecht, The Netherlands. [5]MRC Genome Damage and Stability Centre, University of Sussex, Falmer, Brighton, BN1 9RQ, UK. [6]Hybrigenics Pharma, 75014 Paris, France.

*correspondence: g.s.stewart@bham.ac.uk

Telephone: +44 0121 414 9168

Fax: +44 0121 414 4486

Words:

KEYWORDS

TLS: Translesion synthesis

DDT: DNA damage tolerance

PRR: Post-replication repair

Abstract

Rad18 functions at the cross-roads of three different DNA damage response (DDR) pathways involved in protecting stressed replication forks: homologous recombination repair, DNA inter-strand cross-link repair and DNA damage tolerance. Whilst Rad18 serves to facilitate replication of damaged genomes by promoting translesion synthesis (TLS), this comes at a cost of potentially error-prone lesion bypass. In contrast, loss of Rad18-dependent TLS potentiates the collapse of stalled forks and leads to incomplete genome replication. Given the pivotal nature with which Rad18 governs the fine balance between replication fidelity and genome stability, Rad18 levels and activity have a major impact on genomic integrity. Here, we identify the de-ubiquitylating enzyme USP7 as a critical regulator of Rad18 protein levels. Loss of USP7 destabilises Rad18 and compromises UV-induced PCNA mono-ubiquitylation and Pol η recruitment to stalled replication forks. USP7-depleted cells also fail to elongate nascent daughter strand DNA following UV-irradiation and show reduced DNA damage tolerance. We demonstrate that USP7 associates with Rad18 directly via a consensus USP7-binding motif and can disassemble Rad18-dependent poly-ubiquitin chains both *in vitro* and *in vivo*. Taken together, these observations identify USP7 as a novel component of the cellular DDR involved in preserving genome stability.

Introduction

The ability to recognize and accurately repair damaged DNA is essential for viability. In addition to repair processes that actively remove DNA lesions, cells have evolved mechanisms for tolerating the presence of damaged DNA that interferes with DNA replication. DNA damage tolerance (DDT) mechanisms are important for maintaining ongoing replication of genomes containing unrepaired bulky DNA lesions that block conventional replicative DNA polymerases and disrupt replication fork progression.

It is becoming clear that post-translational modifications and especially ubiquitylation/de-ubiquitylation play a major role in both DNA repair as well as the regulation of DNA damage tolerance during replication (1). For example, bulky DNA lesions e.g. UV-induced cyclobutane pyrimidine dimers that block replicative DNA polymerases and thus stall replication forks, can activate the E3 ubiquitin ligase Rad18, which together with its E2-conjugating enzyme Rad6, catalyzes the mono-ubiquitylation of PCNA on lysine K164 (2-4). This modification of PCNA facilitates the binding of specialized translesion synthesis (TLS) DNA polymerases, which can efficiently synthesize past bulky DNA adducts (5-8). However, Rad18-mediated lesion bypass is inherently error-prone and must be used sparingly in order to avoid mutations. Rad18-deficient cells are TLS-compromised and hypo-mutagenic (9-11) while ectopically over-expressed Rad18 results in DNA damage-independent PCNA mono-ubiquitylation and recruitment of TLS polymerases to replication forks (12, 13). Therefore, appropriate control of Rad18 expression levels is important for balancing replication stress tolerance with mutagenesis.

In addition to regulating protein-protein interactions, ubiquitylation can also alter the stability, localization or functionality of a protein. In this respect, whereas the

mono-ubiquitylation of PCNA increases its interaction with TLS polymerases, the same modification on DNA polymerase eta renders the protein inactive by blocking both its nuclear localization signal and its ability to bind PCNA (6). Similarly, the mono-ubiquitylation of Rad18 has also been proposed to negatively regulate the DNA damage tolerance pathway, through its ability to block its interaction with HLTF and SHPRH (14); two E3 ubiquitin ligases required to carry out error-free bypass of a DNA lesion. Moreover, in contrast to unmodified Rad18, which resides in the nucleus, the mono-ubiquitylated form of Rad18 has been shown to be predominantly localized to the cytoplasm (15), suggesting that this modification may suppress Rad18 activity via multiple different mechanisms.

Removal of ubiquitin from mono- and poly-ubiquitylated proteins is also critical for determining the ubiquitylation state of various E3 ligase substrates. Increasingly, it is becoming clear that de-ubiquitylating (DUB) enzymes play major roles in controlling a wide variety of different cellular processes including the response to DNA damage (16). One DUB that has received a lot of attention, primarily through its well-documented role in controlling the stability of the p53-directed E3 ubiquitin ligases MDM2 and MDMX, is the Herpes associated ubiquitin specific protease, USP7/Hausp. In unstressed cells, USP7 binds to and stabilizes MDM2/MDMX, which in turn promotes the poly-ubiquitylation of p53 and its subsequent destruction by the proteasome (17). Upon induction of DNA damage, the interaction between USP7 and MDM2/MDMX is disrupted (18) by ATM-dependent phosphorylation (19), which functions to promote the ubiquitin-dependent destruction of MDM2/MDMX, thus allowing p53 to accumulate. Originally identified through its association with the Herpes Simplex Virus E3 ligase ICP0, USP7 has been found to regulate the stability of a multitude of different cellular proteins many of which are E3 ubiquitin ligases,

including CHFR and more recently, UHRF1 and HLTF (20-23). In addition to controlling protein stability, USP7 has also been reported to affect both the cellular compartmentalization and activity of a number of its substrates (24).

Here, we identify Rad18 as a novel USP7 binding partner and substrate. USP7-mediated de-ubiquitylation protects Rad18 from proteasomal degradation and is necessary for the integrity of the TLS pathway. Importantly, USP7-deficiency recapitulates key phenotypes of TLS-deficient cells including defective replication of damaged genomes and UV hypersensitivity. Owing to its key roles in multiple DNA damage signaling pathways, USP7 may allow coordination of Rad18-mediated TLS with other branches of the DDR including p53 signaling, Chk1 and Rad5-mediated PRR. Moreover, since Rad18 confers tolerance to chemotherapeutic agents such as cisplatin and camptothecin, our results suggest a rationale for the use of USP7 inhibitors as chemo-sensitizers to treat tumours clinically.

Results

USP7 depletion leads to destabilization of Rad18 protein levels

Given that Rad18 has been shown to undergo poly-ubiquitylation and proteasome-mediated degradation *in vivo* (15), we hypothesised that this poly-ubiquitylation-coupled Rad18 degradation maybe counteracted by a Rad18-targeted de-ubiquitylating activity. To test this hypothesis, we used siRNA to individually deplete a subset of DUBs, previously identified to function in the DNA damage response (16), to determine what impact loss of these DUBs has on the stability of Rad18. Strikingly, we observed that compromising USP7 levels but not those of USP1, USP11, USP3 or USP28, resulted in a significant reduction in the levels of Rad18 (Figure 1A). Importantly, the reduction in Rad18 levels was not due to siRNA

'off-target' effects as we obtained similar results using multiple USP7-directed siRNAs (Figure 1B). Moreover, USP7-/- HCT116 cells expressed reduced levels of Rad18 when compared with the parental (USP7-expressing) HCT116 cells. In addition, pharmacological inhibition of USP7 using HBX19818 also recapitulated the effect of USP7-deficiency on Rad18 expression (Figure 1C). Critically, this reduction of Rad18 protein levels in USP7-deficient cells could not be accounted for by any alterations in either Rad18 mRNA expression or cell cycle distribution (Supplementary Figure 1A and 1B).

Treatment with the proteasome inhibitor MG132 partially rescued the reduced Rad18 protein levels resulting from either siRNA-mediated USP7-depletion (Figure 1D), pharmacological inhibition of USP7 activity (Figure 1E left panel), or inactivation of the *USP7* gene (Figure 1E right panel). Combined, these results indicate that Rad18 is actively degraded by the proteasome in response to loss of USP7 DUB activity. Crucially, re-expression of a siRNA-resistant WT but not a catalytically-inactive ('Dead') mutant USP7 in cells lacking endogenous USP7, substantially restored Rad18 levels demonstrating that the enzymatic activity of USP7 is necessary for maintaining normal Rad18 protein expression (Figure 1F). Taken together, these data demonstrate that USP7 is important for maintaining cellular pools of Rad18 and that upon loss of this protection Rad18 is targeted for proteasomal degradation.

Cells lacking USP7 exhibit defects in the DNA damage tolerance pathway.

Given that loss of USP7 function led to substantial reduction in Rad18 protein levels, we asked whether USP7-depletion would recapitulate hallmarks of Rad18-deficiency. First, we tested the effect of USP7-depletion on DNA damage-induced

mono-ubiquitylation of PCNA, the best-characterized substrate of Rad18. Strikingly, USP7 deficient cells displayed a significant reduction in the levels of UV-induced PCNA mono-ubiquitylation (mUb-PCNA) when compared to cells expressing USP7 (Figure 2A and Supplementary Figure 2).

One critical function of PCNA mono-ubiquitylation is to provide a docking site for TLS polymerases (3, 5, 7, 8, 25, 26), for example DNA Pol η, which binds to mUb-PCNA through its PIP motif, ubiquitin-binding domain (UBZ) and PCNA interacting region (PIR) (3, 6, 7). As shown in Fig. 2B, the UV-induced redistribution of Pol η to sites of replication fork stalling (determined by the quantification of cells with nuclear GFP-Pol η foci) was reduced by 40-60% in USP7-depleted cells relative to control siRNA transfected cells. Importantly, this was not due to an alteration in the levels of Pol η because they remained unaffected by USP7 depletion in multiple cell lines (Supplementary Figure 3).

Due to an inability of replication forks to bypass bulky DNA lesions, DNA damage bypass deficient cells, such as those lacking Rad18, Polη or Rev1, exhibit defective elongation of nascent DNA strands following UV-treatment, termed a post-replication repair (PRR) defect (10, 27, 28). To ascertain whether USP7 knockdown would give rise to deficiency in PRR, we used alkaline sucrose gradient sedimentation centrifugation to determine the effects of USP7-depletion on the elongation rates of newly-replicated DNA in UV-irradiated cells. Notably, the DNA size-distribution profiles in Fig. 2C show that USP7-depleted cells accumulated high molecular mass DNA at a reduced rate compared to control cells. More importantly, this effect was similar but not as severe to that observed in Rad18 deficient cells (Supplementary Figure 4) Therefore, USP7-deficiency leads to decreased chain

elongation following UV-treatment, recapitulating a major phenotype of Rad18/TLS-deficient cells.

USP7 has also been shown to control the stability of HLTF (Supplementary Figure 5A and (23)), which has recently been implicated in potentiating the levels of PCNA mono-ubiquitylation in response to replication stress (29). Therefore, we considered the possibility that HLTF dysregulation may contribute to the TLS-related phenotype we observed in USP7 defective cells. However, despite HLTF expression being knockdown to almost undetectable levels, this had no impact on the levels of UV-induced PCNA mono-ubiquitylation, indicating that reduced HLTF levels in USP7-depleted cells do not account for the attenuation of PCNA mono-ubiquitylation (Supplementary Figure 5B).

It has been shown that a deficiency in Rad18, Rev1 or DNA Polζ-dependent TLS gives rise to a hypo-mutagenic phenotype following UV irradiation (9-11, 30-35) whereas HLTF depletion renders cells hyper-mutagenic (29), Therefore, we determined the effect of USP7-depletion on mutagenesis using a plasmid-based reporter assay (29). As shown in Fig. 2D, USP7-depletion had no effect on spontaneous mutagenesis of an undamaged reporter plasmid. Strikingly, however, the mutation frequency of UV-damaged reporter plasmids was reduced by approximately 50% in USP7-deficient cells when compared to control cells (Figure 2D). This observation is in agreement with the hypo-mutagenic phenotype of Rad18/TLS deficient cells following UV-irradiation (9-11, 30-35) and further indicates that reduced HLTF levels do not account for the PRR defects we observed in cells lacking USP7. Furthermore, consistent with the phenotypes of Rad18/TLS-deficient cells, USP7-depletion conferred a modest hypersensitivity to agents that induce

replication stress (including UV, MMC, and HU) but not IR, which induces DSBs (Figure 2E).

To directly ascertain if a reduction in Rad18 expression is the underlying cause for the sub-optimal UV-induced mono-ubiquitylation of PCNA in USP7 depleted cells, we used an inducible cell system to allow for the controlled re-expression of Rad18 in USP7 siRNA transfected cells. HeLa cells expressing a doxycycline-inducible WT Flag-tagged Rad18 expression construct were transfected with USP7 siRNA and 72 hours following transfection, doxycycline was added to the media for 24 hours. The cells were then UV irradiated, harvested six hours post-irradiation and extracts analyzed by Western blotting (Figure 2F). As expected, in the absence of doxycycline, we found that cells depleted of USP7 exhibited a reduction in levels of PCNA mono-ubiquitylation (compare lane 7 with lane 3). However, this was restored upon re-expression of Rad18 following the addition of doxycycline (compare lane 8 with lane 4). This observation is consistent with the premise that dysregulation of Rad18 levels accounts for the reduced PCNA mono-ubiquitylation in USP7 depleted cells.

Taken together, our results demonstrate that USP7 confers Rad18 stability, and is necessary for Rad18 effector functions in response to the induction of genotoxic stress including Pol η redistribution to sites of UV lesions, replication of damaged genomes, mutagenesis and DNA damage tolerance.

USP7 associates with Rad18 and dismantles Rad18-dependent poly-ubiquitin chains *in vitro and in vivo*.

Since USP7 is implicated in regulating the stability of a number of different substrates, including several E3 ubiquitin ligases, we wished to examine whether the

requirement for USP7 to maintain Rad18 levels was direct or mediated by a USP7-dependent pathway. To determine whether Rad18 and USP7 exist in a complex, we performed reciprocal immunoprecipitations to isolate ectopically co-expressed, epitope-tagged forms of Rad18 and WT or catalytically-inactive (Dead) USP7 from HEK293 cell extracts. Notably, we observed a robust interaction between Rad18 and USP7 that was enhanced when the enzymatic activity of USP7 was ablated (Figure 3A). Moreover, purified, recombinant forms of Rad18 and USP7 could also bind together *in vitro* (Figure 3B) indicative that this interaction is direct.

Given that USP7 and Rad18 associate and that Rad18 auto-ubiquitylation has been proposed to target it for proteasomal degradation (15), we reasoned that the dependence of Rad18 stability on USP7 could be a mediated through its ability to antagonize Rad18 auto-ubiquitylation. To address this, Rad18-dependent auto-ubiquitylation reactions were carried out in the presence or absence of recombinant purified WT and catalytically inactive USP7. Strikingly, the robust auto-ubiquitylation of Rad18, detected with either an anti-Rad18 or anti-poly-ubiquitin (FK2) antibody was completely abolished by the addition of WT but not DUB-dead USP7 (Figure 3C), strongly indicating that USP7 is capable of antagonising the E3 ubiquitin ligase activity of Rad18 *in vitro*. Moreover, the specificity of USP7 activity was verified by the observation that the addition of recombinant USP25 (an irrelevant DUB) to the Rad18 auto-ubiquitylation reaction failed to reverse Rad18-dependent ubiquitin chain formation (Supplementary Figure 6).

To ascertain whether Rad18 poly-ubiquitin chains are also targeted by USP7 *in vivo*, MRC5 cells were transfected with either WT ubiquitin or a mutant ubiquitin harboring a lysine-48 to arginine substitution (designated 'K48R', which cannot form poly-ubiquitin chains), together with either a WT or DUB Dead USP7 mammalian

expression construct. The cells were then treated with MG132 to promote stabilization of poly-ubiquitin chains and a Rad18 antibody was used to detect endogenous poly-ubiquitylated Rad18. As shown in Figure 3D, endogenous Rad18 was modified by K48-linked poly-ubiquitin chains *in vivo* (compare lanes 3 with 5) that was suppressed by the over-expression of WT USP7 (compare lanes 3 with 6) but not by the catalytically-inactive USP7 mutant (compare lanes 6 with 7). These results indicate that USP7 is a novel Rad18-directed DUB that removes K48-linked poly-ubiquitin chains generated via Rad18 auto-ubiquitylation.

Rad18 has a consensus USP7 binding motif required to maintain its stability *in vivo*.

To map the region of Rad18 responsible for mediating its binding to USP7, a panel of overlapping Rad18 fragments fused to GST was incubated with recombinant full length USP7, co-associated proteins were purified on glutathione beads and detected using Western blotting (Figure 4A). Interestingly, these binding studies identified amino acids 110-251 of Rad18 (which encompass the Ubiquitin-Binding Zinc motif) as the USP7-binding domain (Figure 4A).

Notably, the region of Rad18 we identified as being necessary for its interaction with USP7 using *in vitro* binding assays (amino acids 110-251) contained two motifs conforming to the consensus USP7 binding sequence previously identified in other USP7 interacting proteins (P/AxxS: where position +1 is either a proline or alanine, x is any amino acid and position +4 is a serine, which has been shown to be critical for USP7 binding) (36). To ascertain if either of these binding motifs mediates the interaction with USP7, we mutated the consensus serine residues at amino acids 183 or 192/194 of Rad18 to alanine and then repeated the *in vitro* binding assays

with the two mutant Rad18 fragments (Figure 4B). Whereas mutation of the serine at position 183 on Rad18 had no effect on its interaction with USP7 *in vitro*, mutation of the two serines at position 192 and 194 in the second PxxS motif completely abolished USP7-binding (Figure 4B). Co-immunoprecipitation analysis using extracts from 239T cells co-expressing full length USP7 and either WT Rad18 or a S192/194A Rad18 mutant confirmed that the serine residues 192 and 194 in the Rad18 protein are also essential for binding to USP7 *in vivo* (Figure 4C).

More importantly, in keeping with a role for this PxxS motif in modulating the stability of Rad18, analysis of *in vivo* protein half-life using cycloheximide in MRC5 cells revealed that the S192/194A mutant Rad18 is profoundly less stable than its WT counterpart (Figure 4D). Furthermore, the accelerated degradation of this mutant Rad18 was completely abrogated in cells that were previously transfected with USP7 siRNA, indicating that the S192/194A mutation in Rad18 renders it more unstable than the WT protein only in the presence of USP7 (Figure 4E). To ascertain the impact of this mutation on Rad18-dependent functions in response to UV-irradiation, MRC5 cells were first transfected with Rad18 siRNA and 48 hours later were further transfected with either an siRNA-resistant WT or S192/194A HA-tagged RAD18 expression construct or an empty vector. The cells were then UV irradiated and the levels of PCNA mono-ubiquitylation or GFP-Pol η re-localisation were determined by Western blotting (Figure 4F) and immunofluorescence microscopy respectively (Figure 4F). Interestingly, we noted that the S192/194A mutant HA-Rad18, when transiently expressed at similar levels to the WT protein, could efficiently promote both the UV-induced mono-ubiquitylation of PCNA and also the relocalisation of GFP-Pol η to sites of damage. Therefore, we can conclude that the S192/194A Rad18 mutation does not adversely impact Rad18 function directly. However, a

failure to bind USP7 renders the Rad18 S192/194A unstable and as a consequence, compromises its ability to effectively promote both PCNA mono-ubiquitylation and Pol η relocalisation to sites of UV stalled replication.

Discussion

In our study, we identify a novel role for USP7 in regulating an important effector branch of the response to DNA damage, namely TLS. In particular, we demonstrate that the primary mechanism by which USP7 controls this pathway in response to replication damage is by regulating the stability of Rad18; the principal E3 ubiquitin ligase that directs activation of the DNA damage tolerance pathway through its ability to mono-ubiquitylate PCNA. Intracellular Rad18 levels can have a major influence on the activation state of the TLS pathway: reduced Rad18 expression attenuates PCNA mono-ubiquitylation and as a result compromises replication of damaged genomes. Consequently, this can lead to fork collapse, DSB formation and ultimately, cell death (37). In addition, Rad18-deficiency also renders cells hypo-mutagenic (owing to reduced activation of error-prone Y-family polymerases (9-11). Conversely, aberrant high-level expression of Rad18 can promote PCNA mono-ubiquitylation and drive recruitment of Y-family TLS polymerases to replication forks even in the absence of DNA damage (12, 13). This could potentially increase mutation rates and potentiate cellular transformation. Therefore, it is clear that Rad18 expression levels can have a major influence on DNA damage tolerance, mutagenesis and the maintenance of genomic stability.

A recent report by Qian et al. suggested that another component of the TLS pathway, Pol η, is a direct target of USP7-mediated de-ubiquitylation (38). This study

shows that the DUB activity of USP7 promotes the degradation of Pol η by stabilising MDM2, which has been previously reported to poly-ubiquitylate Pol η (39). Furthermore, the authors report that ectopic USP7 over-expression, can lead to increased Pol η stability, which they suggest promotes the mono-ubiquitylation of PCNA following UV irradiation in these cells. Our analysis demonstrates that USP7 depleted cells display reduced levels of Rad18 and as a result, defective PCNA mono-ubiquitylation and Pol η re-localisation following UV-irradiation. In contrast to the observation by Qian et al. that USP7 loss increases Pol η stability, we have not detected any alterations either in Pol η protein levels or Pol η protein turnover in cells lacking USP7 (Supplementary Figures 3 A-D). However, even if Pol η stability is increased upon USP7 loss, based on our data, it would still not relocalise efficiently to sites of stalled replication in these cells (Figure 2B). Moreover, the restoration of PCNA mono-ubiquitylation in USP7 deficient cells by the re-expression of Rad18 (Figure 2F), further indicates that it is unlikely that the changes in PCNA mono-ubiquitylation levels are due to increased Pol η stability.

Although Rad18 function has been studied extensively, surprisingly little is known about how its expression levels are regulated. Our work underlines the importance of USP7 for Rad18 stability and as such for efficient DNA damage bypass. We have identified a consensus USP7 binding motif in Rad18 that protects the protein from accelerated degradation. Yamaizumi and colleagues demonstrated that Rad18 can poly-ubiquitylate itself and that this modified form of Rad18 can be targeted for degradation by the proteasome (15). Our study identifies USP7 as a novel Rad18-directed DUB that removes poly-ubiquitin chains and antagonizes the proteasomal degradation of Rad18. However, whether the poly-ubiquitin-directed degradation of Rad18 is driven solely by its auto-ubiquitylation, remains unclear.

Unfortunately, due to the inherent instability of catalytically-inactive Rad18 RING domain mutants (40) we have been unable to ascertain whether Rad18 poly-ubiquitylation can occur independently of its catalytic activity. Moreover, we cannot rule out the involvement of other, as yet unidentified E3 ligases, contributing to the poly-ubiquitylation and subsequent degradation of Rad18.

In addition to poly-ubiquitylation, Rad18 is also mono-ubiquitylated in mammalian cells. Interestingly, in many of our experiments it appeared that the unmodified form of Rad18 is more susceptible to degradation in the absence of USP7 than the mono-ubiquitylated form. It is tempting to speculate that the mono-ubiquitylation of Rad18 makes it more resistant to poly-ubiquitylation and proteasomal-dependent degradation. In support of this, it has been shown that the mono-ubiquitylated form of Rad18 is almost exclusively localised in the cytoplasm (15) whereas in contrast, USP7 is primarily localised in the nucleus (41). As such, this could provide one explanation for the differential sensitivity of the unmodified versus mono-ubiquitylated forms of Rad18 to loss of USP7. Intriguingly, we also observed that even when USP7 is completely absent, the levels of Rad18 protein are never completely depleted. Whilst the underlying reason for this is unknown, this is consistent with a specific pool of Rad18, perhaps the mono-ubiquitylated form, being somehow protected from degradation and as such does not require the de-ubiquitylating activity of USP7. Moreover, since it is known that Rad18 exists as a dimer, it is possible that the unmodified Rad18 remaining in cells lacking USP7 is safeguarded from degradation through its association with a mono-ubiquitylated molecule of Rad18. In keeping with this, we repeatedly observed that the ratio of unmodified to mono-ubiquitylated forms in USP7 deficient cells shifted from a predomination of the unmodified form to stoichiometric amounts of both forms.

Recently, it has been suggested that the ubiquitylated form of Rad18 is inactive (14). It was proposed that the mono-ubiquitylation of Rad18 is required to mediate its dimerisation with another (unmodified) molecule of Rad18 resulting in its inactivation. However, following the induction of replication damage, the Rad18 dimer becomes de-ubiquitylated and subsequently activated. This observation highlights the point that regulating Rad18 ubiquitylation also plays a key role in controlling its activity. Currently, it is not clear whether USP7 contributes to the DNA damage-inducible removal of the mono-Ub from the inactive Rad18 homo-dimer, although at least *in vitro*, USP7 is capable of completely de-ubiquitylating Rad18. Interestingly, when we over-expressed USP7 super-physiological levels in cells, rather than increasing the stability of Rad18, we observed a reduction in the mono-ubiquitylated form of Rad18. It is therefore possible that the elevated level of UV-induced PCNA mono-ubiquitylation in cells over-expressing USP7 reported by Qian et al. is mediated through the de-ubiquitylation and activation of Rad18.

Since we have shown that USP7 is essential for maintaining Rad18 stability in cells and that loss of USP7 phenocopies the hallmark DDT defects associated with Rad18 deficiency, one inference from our work is that compromising USP7 function would be sufficiently detrimental to genomic integrity that it could potentiate cellular transformation. Interestingly, it has been recently demonstrated that a significant proportion of paediatric T cell acute lymphoblastic leukaemia (ALL) tumour samples have acquired somatic, loss-of-function mutations in *USP7* (42). Since ablating USP7 function results in p53 stabilisation and an increase in p53-dependent G1 arrest and/or apoptosis, it is somewhat difficult to rationalize how these mutations would be beneficial for tumourigenesis unless they are acquired in tumour cells that already have an inactivated the p53 pathway. However, it is tempting to speculate that

compromised Rad18-dependent DNA damage tolerance in USP7-defective tumour cells could permit the accumulation of DNA DSBs induced by replication stress, which if repaired inappropriately by non-homologous end-joining pathways, would give rise to the formation of gross genomic rearrangements; a process known to be necessary for transformation and/or disease progression.

Despite that USP7 has been shown to be important for regulating the stability of a number of different cellular proteins, its link to the p53 pathway has been the principal driver for the development of inhibitors to be used as anti-cancer treatments. However, since inhibiting USP7 primarily induces p53-dependent cell death, it is plausible that the frequent inactivation of *TP53* would allow tumour cells to resist cell death following USP7 loss. In spite of this, our data suggests that USP7 inhibition could nevertheless sensitise tumours, (including those lacking functional p53), to genotoxic therapeutic agents such as cisplatin (43) or camptothecin (44) that are normally tolerated by cancer cells via Rad18-dependent mechanisms. As a consequence this work suggests that the potential therapeutic use of USP7 inhibitors could be widened to include those tumours with a defective p53 pathway, especially if combined with conventional chemotherapeutic agents.

Materials and Methods

Cell culture

HeLa, U2OS, 293T cells (ATCC) and 293FT (Invitrogen) were maintained in DMEM (Gibco, Invitrogen) supplemented with 10% foetal calf serum (FCS), glutamine and penicillin/streptomycin (pen/strep) at 37°C in 5% CO_2. USP7 WT and knockout HCT116 cells were maintained in RPMI1640 (Gibco, Invitrogen) supplemented with 10% foetal calf serum (FCS), glutamine and penicillin/streptomycin (pen/strep) at 37°C in 5% CO_2. MRC5-SV40 cells were maintained in MEM supplemented with 10% foetal calf serum (FCS) and glutamine. Flp-In/T-rex HeLa cells were a kind gift from Dr. Jakob Nilsson and maintained in DMEM supplemented with 10% FCS, glutamine, 200µg/ml hygromycin and 5µg/ml blasticidin. XP30RO (XP-Variant) or XP30R0 stably expressing *POLH* cDNA [$XP30RO^{poln}$] (45) were a kind gift from Dr. Patricia Kannouche and were maintained in MEM supplemented with 10% foetal calf serum (FCS) and glutamine.

Chemicals/Inhibitors

Doxycycline (used at 200ng/ml) was purchased from Sigma. Cycloheximide used at used at 60µg/ml was purchased from Merck Millipore. The USP7 inhibitor HBX19818 was kindly provided by Dr. Frédéric Colland (Hybrigenics) and has been previously reported elsewhere (46, 47).

Plasmids

The GFP- and Flag-tagged USP7 expression constructs were obtained from Dr. Madelon Maurice and have been previously described elsewhere (19). The pEGFP- and Flag-*Rad18* expression constructs were a kind gift from Drs. Akira

Yasui, Jun Huang and Junjie Chen and have been previously published (48, 49). The plasmids encoding overlapping fragments of Rad18 fused to GST have been previously described (50). Introduction of the S192/194A mutation in the *RAD18* ORF was achieved using the site-directed mutagenesis kit (Stratagene) according to the manufacturer's instructions using the following primers Forward: CGT CCT GAG CCA CCC GCG ACA GCC ACT TTG AAA CAA GTT ACT and Reverse: AGT AAC TTG TTT CAA AGT GGC TGT CGC GGG TGG CTC AGG ACG. For the introduction of the S183A mutation the primers used were: Forward: AA GAG ATC GCT CCA GAT CCC GCA GAG GCT AAG, Reverse: CTT AGC CTC TGC GCG ATC TGG AGC GAT CTC TT. Expression constructs for GFP-pol η and HA-tagged wt Rad18 were kindly provided by Dr. Patricia Kannouche.

Antibodies and Western Blotting

The anti-USP7, SMC1, Rad18, Rad6, HLTF, USP1, USP11, USP3 and USP28 antibodies were all purchased from Bethyl. The histone H2A (acidic patch) antibodies were obtained from Millipore. Antibodies to PCNA, cyclin A, Cdt1 and Rad51 were obtained from Santa-Cruz. The anti-Rad18, anti-Polη and β-Tubulin antibodies were all purchased from Abcam and the anti-poly-ubiquitin (FK2) antibody was obtained from Biomol. The anti-Flag (M2), β-actin and anti-HA epitope tag antibodies were purchased from Sigma. The anti-GFP (living colours) antibody was obtained from Clontech.

siRNA and transfections

The siRNA duplexes were all 21 base pairs with a 2-base deoxynucleotide overhang. The sequence of the custom USP7 and control siRNA oligonucleotides

used were: CCCAAATTATTCCGCGGCAAAdTdT and CGUACGCGGAAUACUUCGAdTdT respectively (Thermo Fisher). The Claspin, HLTF, USP1, USP3, USP11, USP28, DNA polymerase η (Polη) and USP7 (AAGCGUCCCUUUAGCAUUAUU, GCAUAGUGAUAAACCUGUAUU, UAAGGACCCUGCAAAUUAUUU, and GUAAAGAAGUAGACUAUCGUU) siRNA on-target plus SMARTpools and human RAD18 individual on-target plus oligonucleotide (GAAAUGAGUGGUUCUACAU**)** were all purchased from Thermo Fisher. Cells were transfected with siRNA duplexes using Oligofectamine (Invitrogen), following the manufacturer's instructions. Cells were routinely harvested 72h after siRNA transfection. HeLa cells were transfected with a siRNA resistant Flag-*USP7* expression construct using Lipofectamine 2000 according to the manufacturer's instructions.

Immunofluorescence

Following siRNA and pEGFP-*Pol η* transfections, HeLa or MRC5 cells were seeded onto coverslips and mock-irradiated or UV-irradiated. Cells were washed twice in PBS, fixed in 3.6% paraformaldehyde at room temperature for 20 min and were then sealed with vectashield containing DAPI (Vectorlabs). All slides were analyzed by fluorescence microscopy at x60 magnification (Nikon E600).

Colony survival.

Cells transfected with siRNA were seeded at low density and exposed to a variety of DNA damaging agents. Cells were left for 14 days at 37°C to allow colonies to form. Colonies were stained with 2% methylene blue/50% ethanol and counted. Colonies were defined as containing 50 or more cells.

Post-replication repair assay.

The assay was performed as previously described with minor modifications (6).

Mutagenesis assay.

293T cells were transfected with non-target control or USP7-directed siRNAs using Lipofectamine 2000. 24 h later, the cells were transfected with an undamaged or UV-irradiated pSP189 reporter plasmid (Parris and Seidman, 1992) using Lipofectamine 2000. After 48 h, the pSP189 plasmid was recovered from the 293T cells using a DNA miniprep kit (QIAGEN). Purified plasmid DNA was DpnI-digested and electroporated into the MBM7070 bacterial strain. The mutation frequency in the SupF coding region was determined by enumerating the ratios of blue (wild-type) and white (mutant) colonies.

Immunoprecipitation

293FT cells transfected with epitope tagged USP7 and Rad18 expression constructs were lysed for 30 minutes in NETN lysis buffer (50mM Tris/HCl pH 7.5, 150mM NaCl, 1mM EDTA, 2mM $MgCl_2$, 1% NP40 supplemented with protease inhibitors (Roche) and Benzonase (Novagen). The clarified extract was pre-cleared with the appropriate IgG (Dako) and protein A or G beads (GE Healthcare) for 1 h at 4˚C. Immuno-precipitating antibody (10 μg) was added to the pre-cleared supernatant for 2.5 hours followed by protein A or G beads and incubated for 1.5h at 4˚C. The immuno-complexes were washed four times in NETN lysis buffer (containing 0.5% NP40), boiled in SDS sample buffer and loaded on an SDS–

polyacrylamide gel. Proteins were analyzed by Western blotting using standard methods and detected with the antibodies described above.

In vitro protein binding assay

All reactions were conducted at 4°C unless otherwise stated. Immunoprecipitations using purified proteins were carried out as follows: 500ng of purified USP7 (BostonBiochem) and Rad18 (ORIGENE) were mixed for 2 hours at 4˚C in a 500µl reaction with NETN buffer (50mM Tris pH 7.5, 1mM EDTA, 150mM NaCl and 0.5% NP-40) supplemented with a complete protease inhibitor cocktail (Roche). After this incubation, the reactions were span down at 44,000 rpm for 15 min at 4˚C and the supernatants were incubated with 0.5µg of USP7 or Rad18 (Bethyl) or rabbit IgG (DAKO) polyclonal antibodies in separate reactions overnight. The following day, the reactions were span down at 13,000 rpm for 5 min and the supernatants were mixed with 20µl of protein A beads and left on a carousel for 2 hours. The reactions were span down at 3,000 rpm for 2min and the supernatants discarded. The beads were washed three times in 1ml NETN buffer (once in NETN with 150mM NaCl followed by two washes in NETN with 400mM NaCl) and were then re-suspended in 40µl SDS sample buffer and boiled for 5min at 95˚C.

GST-pulldowns

All reactions were carried out at 4°C unless otherwise stated. Equal amounts of GST-Rad18 protein fragments were mixed each with 500ng of purified His-tagged USP7 (Caltag Medsystems) in 500µl of NETN buffer (50mM Tris pH 7.5, 1mM EDTA, 150mM NaCl and 1% NP-40) supplemented with complete protease inhibitor cocktail tablets (Roche) for 1 hour and were then span down at 13,000rpm for a min. The

supernatants were incubated for 1 hour with 20µl of GST-beads (per reaction) previously washed in the same buffer. After this incubation, the reactions were span down at 3,000 rpm for 2min and the supernatants discarded. The beads were then washed five times in 1ml NETN buffer and were then re-suspended in 40µl SDS sample buffer and boiled for 5min at 95˚C.

***In vitro* ubiquitylation/de-ubiquitylation assays.**

0.2µg of E1, 0.5µg of E2 (Rad6), 0.5µg of the E3 (Rad18) and 5µg of ubiquitin were all mixed in a ubiquitylation reaction buffer containing 50mM Tris pH7.5, 5mM $MgCl_2$, 1mM DTT and 1xATP regeneration buffer (Enzo Life Sciences) in a final volume of 20µl for 3 hours at 37°C. For de-ubiquitylation assays, after the 3 hour ubiquitylation reaction, increasing amounts (0.5µg, 1µg, 1.5µg) of purified USP7 (Caltag Medsystems) or 0.5µg of recombinant WT or catalytically inactive (C223S) USP7 (A generous gift from Chris Boutell and Roger Everett) or WT USP25 (Enzo Life Sciences) were added to the mix (final volume of 30µl) and the reactions were further incubated for 2 hours at 37°C. In all cases reactions were terminated by the addition of SDS loading buffer and boiling for 10 min at 95°C.

Flow cytometry

PI analysis: Cells were stained with propidium iodide (PI) as previously described (51) and were analyzed by flow cytometry on an Accuri C6 flow cytometer (BD Biosciences) using the manufacturer's software.

Quantitative RT-PCR (Q-PCR)

RNA was extracted using RNeasy kit (Qiagen, Hilden, Germany) and complementary DNA was generated using Superscript II reverse transcriptase (Life Technologies). SYBR Green quantitative Real-time PCR (Life Technologies) was applied with primers against *RAD18* (Fw: 5'- GCTTCTGGTGGATCAGGCTA-3', Rev: 5'- TCAGGTTCCAATTCCTCTGG-3'). Primers against β-*ACTIN* (Fw: 5'-CACCATTGGCAATGAGCGGTTC, Rev: 5'-AGGTCTTTGCGGATGTCCACGT-3') were used for normalisation and quantification was achieved using the comparative Ct method (52).

Acknowledgments

We are very grateful to Drs. Akira Yasui, Jun Huang, Justin Leung, Junjie Chen and Patricia Kannouche for the kind gift of various Rad18 expression plasmids. We would like to express our thanks to Drs. Jan van der Knaap, Chris Boutell and Roger Everett for providing recombinant purified WT and catalytically inactive USP7 and Dr. Jakob Nilsson for providing the HeLa Flp-In/T-Rex cells. We would also like to thank Dr Malcolm Taylor for critical reading of the manuscript. This work was funded by a Lister Institute Research Prize (AZ and GS), a WWCR project grant (AZ and GS; 13-1012), a CR-UK Senior Research Fellowship (GS and EM; C17183/A13030) and a LLR program grant (AA and TS; 11045), SS was supported by an AIRC Grant 12710 and a 7th Framework Program (CIG 303806). Lastly, we would like to thank the University of Birmingham for supporting this work.

Conflict of Interest

The authors declare no competing financial interests.

REFERENCES

1. Bergink S, Jentsch S. Principles of ubiquitin and SUMO modifications in DNA repair. Nature. 2009;458(7237):461-7. Epub 2009/03/28.
2. Hoege C, Pfander B, Moldovan GL, Pyrowolakis G, Jentsch S. RAD6-dependent DNA repair is linked to modification of PCNA by ubiquitin and SUMO. Nature. 2002;419(6903):135-41. Epub 2002/09/13.
3. Kannouche PL, Wing J, Lehmann AR. Interaction of human DNA polymerase eta with monoubiquitinated PCNA: a possible mechanism for the polymerase switch in response to DNA damage. Mol Cell. 2004;14(4):491-500. Epub 2004/05/20.
4. Watanabe K, Tateishi S, Kawasuji M, Tsurimoto T, Inoue H, Yamaizumi M. Rad18 guides poleta to replication stalling sites through physical interaction and PCNA monoubiquitination. EMBO J. 2004;23(19):3886-96. Epub 2004/09/11.
5. Bomar MG, D'Souza S, Bienko M, Dikic I, Walker GC, Zhou P. Unconventional ubiquitin recognition by the ubiquitin-binding motif within the Y family DNA polymerases iota and Rev1. Mol Cell. 2010;37(3):408-17. Epub 2010/02/18.
6. Bienko M, Green CM, Sabbioneda S, Crosetto N, Matic I, Hibbert RG, et al. Regulation of translesion synthesis DNA polymerase eta by monoubiquitination. Mol Cell. 2010;37(3):396-407. Epub 2010/02/18.
7. Bienko M, Green CM, Crosetto N, Rudolf F, Zapart G, Coull B, et al. Ubiquitin-binding domains in Y-family polymerases regulate translesion synthesis. Science. 2005;310(5755):1821-4. Epub 2005/12/17.
8. Garg P, Burgers PM. Ubiquitinated proliferating cell nuclear antigen activates translesion DNA polymerases eta and REV1. Proc Natl Acad Sci U S A. 2005;102(51):18361-6. Epub 2005/12/14.
9. Hashimoto K, Cho Y, Yang IY, Akagi J, Ohashi E, Tateishi S, et al. The vital role of polymerase zeta and REV1 in mutagenic, but not correct, DNA synthesis across benzo[a]pyrene-dG and recruitment of polymerase zeta by REV1 to replication-stalled site. J Biol Chem. 2012;287(12):9613-22. Epub 2012/02/04.
10. Tateishi S, Niwa H, Miyazaki J, Fujimoto S, Inoue H, Yamaizumi M. Enhanced genomic instability and defective postreplication repair in RAD18 knockout mouse embryonic stem cells. Molecular and cellular biology. 2003;23(2):474-81. Epub 2003/01/02.
11. Yoon JH, Prakash S, Prakash L. Requirement of Rad18 protein for replication through DNA lesions in mouse and human cells. Proc Natl Acad Sci U S A. 2012;109(20):7799-804. Epub 2012/05/02.
12. Bi X, Barkley LR, Slater DM, Tateishi S, Yamaizumi M, Ohmori H, et al. Rad18 regulates DNA polymerase kappa and is required for recovery from S-phase checkpoint-mediated arrest. Molecular and cellular biology. 2006;26(9):3527-40. Epub 2006/04/14.
13. Bekes M, Okamoto K, Crist SB, Jones MJ, Chapman JR, Brasher BB, et al. DUB-resistant ubiquitin to survey ubiquitination switches in mammalian cells. Cell reports. 2013;5(3):826-38. Epub 2013/11/12.
14. Zeman MK, Lin JR, Freire R, Cimprich KA. DNA damage-specific deubiquitination regulates Rad18 functions to suppress mutagenesis. J Cell Biol. 2014;206(2):183-97. Epub 2014/07/16.
15. Miyase S, Tateishi S, Watanabe K, Tomita K, Suzuki K, Inoue H, et al. Differential regulation of Rad18 through Rad6-dependent mono- and polyubiquitination. J Biol Chem. 2005;280(1):515-24. Epub 2004/10/29.

16. Jacq X, Kemp M, Martin NM, Jackson SP. Deubiquitylating enzymes and DNA damage response pathways. Cell Biochem Biophys. 2013;67(1):25-43. Epub 2013/05/29.
17. Li M, Brooks CL, Kon N, Gu W. A dynamic role of HAUSP in the p53-Mdm2 pathway. Mol Cell. 2004;13(6):879-86. Epub 2004/04/01.
18. Meulmeester E, Maurice MM, Boutell C, Teunisse AF, Ovaa H, Abraham TE, et al. Loss of HAUSP-mediated deubiquitination contributes to DNA damage-induced destabilization of Hdmx and Hdm2. Mol Cell. 2005;18(5):565-76. Epub 2005/05/27.
19. Meulmeester E, Pereg Y, Shiloh Y, Jochemsen AG. ATM-mediated phosphorylations inhibit Mdmx/Mdm2 stabilization by HAUSP in favor of p53 activation. Cell Cycle. 2005;4(9):1166-70. Epub 2005/08/06.
20. Canning M, Boutell C, Parkinson J, Everett RD. A RING finger ubiquitin ligase is protected from autocatalyzed ubiquitination and degradation by binding to ubiquitin-specific protease USP7. J Biol Chem. 2004;279(37):38160-8. Epub 2004/07/13.
21. Oh YM, Yoo SJ, Seol JH. Deubiquitination of Chfr, a checkpoint protein, by USP7/HAUSP regulates its stability and activity. Biochem Biophys Res Commun. 2007;357(3):615-9. Epub 2007/04/20.
22. Felle M, Joppien S, Nemeth A, Diermeier S, Thalhammer V, Dobner T, et al. The USP7/Dnmt1 complex stimulates the DNA methylation activity of Dnmt1 and regulates the stability of UHRF1. Nucleic Acids Res. 2011;39(19):8355-65. Epub 2011/07/13.
23. Qing P, Han L, Bin L, Yan L, Ping WX. USP7 regulates the stability and function of HLTF through deubiquitination. J Cell Biochem. 2011;112(12):3856-62. Epub 2011/08/17.
24. Nicholson B, Suresh Kumar KG. The multifaceted roles of USP7: new therapeutic opportunities. Cell Biochem Biophys. 2011;60(1-2):61-8. Epub 2011/04/07.
25. Guo C, Tang TS, Bienko M, Parker JL, Bielen AB, Sonoda E, et al. Ubiquitin-binding motifs in REV1 protein are required for its role in the tolerance of DNA damage. Molecular and cellular biology. 2006;26(23):8892-900. Epub 2006/09/20.
26. Wood A, Garg P, Burgers PM. A ubiquitin-binding motif in the translesion DNA polymerase Rev1 mediates its essential functional interaction with ubiquitinated proliferating cell nuclear antigen in response to DNA damage. J Biol Chem. 2007;282(28):20256-63. Epub 2007/05/23.
27. Lehmann AR, Kirk-Bell S, Arlett CF, Paterson MC, Lohman PH, de Weerd-Kastelein EA, et al. Xeroderma pigmentosum cells with normal levels of excision repair have a defect in DNA synthesis after UV-irradiation. Proc Natl Acad Sci U S A. 1975;72(1):219-23. Epub 1975/01/01.
28. Jansen JG, Tsaalbi-Shtylik A, Hendriks G, Gali H, Hendel A, Johansson F, et al. Separate domains of Rev1 mediate two modes of DNA damage bypass in mammalian cells. Molecular and cellular biology. 2009;29(11):3113-23. Epub 2009/04/01.
29. Lin JR, Zeman MK, Chen JY, Yee MC, Cimprich KA. SHPRH and HLTF act in a damage-specific manner to coordinate different forms of postreplication repair and prevent mutagenesis. Mol Cell. 2011;42(2):237-49. Epub 2011/03/15.
30. Kim H, Yang K, Dejsuphong D, D'Andrea AD. Regulation of Rev1 by the Fanconi anemia core complex. Nat Struct Mol Biol. 2012;19(2):164-70. Epub 2012/01/24.
31. Lawrence CW, Christensen R. UV mutagenesis in radiation-sensitive strains of yeast. Genetics. 1976;82(2):207-32. Epub 1976/02/01.
32. Larimer FW, Perry JR, Hardigree AA. The REV1 gene of Saccharomyces cerevisiae: isolation, sequence, and functional analysis. Journal of bacteriology. 1989;171(1):230-7. Epub 1989/01/01.
33. Gibbs PE, Wang XD, Li Z, McManus TP, McGregor WG, Lawrence CW, et al. The function of the human homolog of Saccharomyces cerevisiae REV1 is required for

mutagenesis induced by UV light. Proc Natl Acad Sci U S A. 2000;97(8):4186-91. Epub 2000/04/13.
34. Gan GN, Wittschieben JP, Wittschieben BO, Wood RD. DNA polymerase zeta (pol zeta) in higher eukaryotes. Cell research. 2008;18(1):174-83. Epub 2007/12/25.
35. McNally K, Neal JA, McManus TP, McCormick JJ, Maher VM. hRev7, putative subunit of hPolzeta, plays a critical role in survival, induction of mutations, and progression through S-phase, of UV((254nm))-irradiated human fibroblasts. DNA repair. 2008;7(4):597-604. Epub 2008/02/26.
36. Sheng Y, Saridakis V, Sarkari F, Duan S, Wu T, Arrowsmith CH, et al. Molecular recognition of p53 and MDM2 by USP7/HAUSP. Nat Struct Mol Biol. 2006;13(3):285-91. Epub 2006/02/14.
37. Zeman MK, Cimprich KA. Causes and consequences of replication stress. Nat Cell Biol. 2014;16(1):2-9. Epub 2013/12/25.
38. Qian J, Pentz K, Zhu Q, Wang Q, He J, Srivastava AK, et al. USP7 modulates UV-induced PCNA monoubiquitination by regulating DNA polymerase eta stability. Oncogene. 2014. Epub 2014/12/02.
39. Jung YS, Qian Y, Chen X. DNA polymerase eta is targeted by Mdm2 for polyubiquitination and proteasomal degradation in response to ultraviolet irradiation. DNA repair. 2012;11(2):177-84. Epub 2011/11/08.
40. Masuda Y, Suzuki M, Kawai H, Suzuki F, Kamiya K. Asymmetric nature of two subunits of RAD18, a RING-type ubiquitin ligase E3, in the human RAD6A-RAD18 ternary complex. Nucleic Acids Res. 2012;40(3):1065-76. Epub 2011/10/05.
41. Everett RD, Meredith M, Orr A, Cross A, Kathoria M, Parkinson J. A novel ubiquitin-specific protease is dynamically associated with the PML nuclear domain and binds to a herpesvirus regulatory protein. EMBO J. 1997;16(7):1519-30. Epub 1997/04/01.
42. Huether R, Dong L, Chen X, Wu G, Parker M, Wei L, et al. The landscape of somatic mutations in epigenetic regulators across 1,000 paediatric cancer genomes. Nature communications. 2014;5:3630. Epub 2014/04/09.
43. Wagner JM, Karnitz LM. Cisplatin-induced DNA damage activates replication checkpoint signaling components that differentially affect tumor cell survival. Molecular pharmacology. 2009;76(1):208-14. Epub 2009/05/01.
44. Palle K, Vaziri C. Rad18 E3 ubiquitin ligase activity mediates Fanconi anemia pathway activation and cell survival following DNA Topoisomerase 1 inhibition. Cell Cycle. 2011;10(10):1625-38. Epub 2011/04/12.
45. Stary A, Kannouche P, Lehmann AR, Sarasin A. Role of DNA polymerase eta in the UV mutation spectrum in human cells. J Biol Chem. 2003;278(21):18767-75. Epub 2003/03/20.
46. Reverdy C, Conrath S, Lopez R, Planquette C, Atmanene C, Collura V, et al. Discovery of specific inhibitors of human USP7/HAUSP deubiquitinating enzyme. Chem Biol. 2012;19(4):467-77. Epub 2012/04/24.
47. Colland F, Formstecher E, Jacq X, Reverdy C, Planquette C, Conrath S, et al. Small-molecule inhibitor of USP7/HAUSP ubiquitin protease stabilizes and activates p53 in cells. Mol Cancer Ther. 2009;8(8):2286-95. Epub 2009/08/13.
48. Huang J, Huen MS, Kim H, Leung CC, Glover JN, Yu X, et al. RAD18 transmits DNA damage signalling to elicit homologous recombination repair. Nat Cell Biol. 2009;11(5):592-603. Epub 2009/04/28.
49. Nakajima S, Lan L, Kanno S, Usami N, Kobayashi K, Mori M, et al. Replication-dependent and -independent responses of RAD18 to DNA damage in human cells. J Biol Chem. 2006;281(45):34687-95. Epub 2006/09/19.

50. Day TA, Palle K, Barkley LR, Kakusho N, Zou Y, Tateishi S, et al. Phosphorylated Rad18 directs DNA polymerase eta to sites of stalled replication. J Cell Biol. 2010;191(5):953-66. Epub 2010/11/26.
51. Zlatanou A, Despras E, Braz-Petta T, Boubakour-Azzouz I, Pouvelle C, Stewart GS, et al. The hMsh2-hMsh6 complex acts in concert with monoubiquitinated PCNA and Pol eta in response to oxidative DNA damage in human cells. Mol Cell. 2011;43(4):649-62. Epub 2011/08/23.
52. Schmittgen TD, Livak KJ. Analyzing real-time PCR data by the comparative C(T) method. Nature protocols. 2008;3(6):1101-8. Epub 2008/06/13.

FIGURE LEGENDS

Figure 1 Rad18 protein levels are reduced in USP7 deficient cells and can be restored by proteasomal inhibition. A HeLa cells were transfected with control siRNA or siRNA against USP7, USP1, USP28, USP3 or USP11. The cells were harvested and extracts from these cells were subjected to Western blotting using the antibodies indicated. **B** HeLa cells were transfected with control siRNA, a single siRNA sequence targeting USP7 or a SMARTpool of USP7 siRNA sequences. The cells were harvested and extracts from these cells were subjected to Western blotting using the antibodies indicated. The loading control is a non-specific band recognized by the anti-Rad18 antibody. **C** HeLa cells were incubated with increasing amounts of a specific USP7 inhibitor (HBX19818) for 24 hours and the levels of USP7 and Rad18 monitored by Western blotting (left panel). The loading control is a non-specific band recognized by Rad18 antibodies. The expression of Rad18 and USP7 was determined by Western blotting on extracts derived from HCT116 cells either expressing USP7 (WT USP7) or in which *USP7* had been knocked out ($USP7^{-/-}$) (right panel). SMC1 was used as a loading control. **D** MRC5 cells were transfected with a single siRNA sequence targeting USP7 as in part 'B' and then incubated with MG132 for the indicated times. Extracts from these cells were subjected to SDS-Page and Western blotting with the antibodies indicated. **E** MRC5 cells were

incubated with 15μM of the USP7 inhibitor (HBX19818) for 16 or 24 hours in the presence or absence of 10μM MG132. The levels of USP7, Rad18 and H2A were monitored by Western blotting (left panel). USP7$^{-/-}$ cells were incubated in media containing either DMSO or MG132 and the levels of Rad18 determined by Western blotting (right panel). Rad51 and Rad6 were used as loading controls. **F** HeLa cells were transfected with control or USP7 siRNA in conjunction with an empty vector, Flag-tagged WT *USP7* or a catalytically dead *USP7* mammalian expression construct. Extracts from these cells were subjected SDS-Page and Western blotting with the antibodies indicated.

Figure 2 USP7 depleted cells fail to activate DNA damage tolerance following UV and phenocopy Rad18 deficient cells. A MRC5 cells were transfected with control or USP7 siRNA, UV-irradiated with 20J/m^2 and then harvested at the times indicated. Extracts from these cells were subjected to SDS-Page and Western blotting with the indicated antibodies. **B** MRC5 cells stably expressing EGPF-Polη were transfected with control or USP7 targeted siRNA in conjunction with a plasmid encoding pEGFP-*Polη*. The cells were mock-irradiated or UV-irradiated with 15J/m^2 and the number of cells with Polη foci was determined. Representative microscopy images are depicted (top) together with quantification of the percentage of EGFP positive cells with Polη foci (bottom). **C** HeLa cells transfected with control or USP7 siRNA were pulse-labeled with ^{3}H-Thymidine, mock-treated or UV-irradiated, and then genomic DNA was extracted. ^{3}H-Thymidine was measured using scintillation counter on fractions obtained from differential sucrose sedimentation centrifugation of the genomic DNA (gDNA). The blue and red curves denote the size of gDNA fragments obtained from UV irradiated cells transfected with either control or USP7

siRNA respectively. The inset graph represents an estimation of the average DNA molecular weight across the distribution normalized to the control siRNA. **D** The mutation frequency was assessed 48 hrs after cotransfection of 293T cells with mock-treated or UV-irradiated plasmid (pSP189) and the indicated siRNAs. The data represent average +/- SEM (shown as error bar) from at least three independent experiments. **E** HeLa cells were transfected with control siRNA or siRNA against USP7 and were then exposed to ionizing radiation (IR), hydroxyurea (HU), mitomycin C (MMC) or ultraviolet radiation (UV) at the doses indicated. The cells were then left for 14 days at 37°C to allow colonies to form. Colonies were defined as containing 50 or more cells. **F** HeLa Flp-In/T-Rex cells expressing Flag-tagged WT RAD18 were transfected with USP7 siRNA, incubated with doxycycline to promote induction of Rad18 expression and then either mock-irradiated or UV-irradiated with 30J/m^2 and the levels of USP7, Rad18 and PCNA were monitored with the indicated antibodies. The asterisk denotes a non-specific band.

Figure 3 USP7 associates with and deubiquitylates Rad18 *in vitro* and *in vivo*. **A** 293FT cells were transfected with plasmids encoding EGFP-*RAD18* and either wild-type (WT) or catalytically inactive (C223S) (DEAD) Flag-*USP7*. USP7 or Rad18 were immunoprecipitated from cell extracts using the indicated antibodies. The immuno-precipitated material was subjected to SDS-Page/Western blotting and the co-associated proteins detected with the indicated antibodies. **B** Purified Flag-tagged USP7 was incubated with purified Rad18 and immunoprecipitations were carried out using antibodies to either USP7 or Rad18. The immuno-precipitated material was subjected to SDS-Page/Western blotting and the co-associated proteins detected with the indicated antibodies. **C** Combinations of an E1 enzyme, an E2 enzyme

(Rad6), Rad18 and ubiquitin were mixed and incubated for 3 hours at 37°C. For de-ubiquitylation assays, after the 3 hour ubiquitylation reaction, either recombinant WT or recombinant catalytically inactive (C223S) USP7 were added to the mix and the reactions were further incubated for 2 hours at 37°C. In all cases the reactions were terminated by the addition of Laemli buffer and boiling for 10 min at 95°C. The proteins were detected using the indicated antibodies. **D** MRC5 cells were transfected with plasmids encoding either WT or K48R *ubiquitin* (lanes 3-7), in some cases with Flag-tagged *RAD18* (lanes 2 and 4) and either WT or catalytically inactive Flag-tagged *USP7* (lanes 6 and 7 respectively) and then incubated in MG132. Extracts from these cells were blotted for Rad18, Flag-USP7 and β-Tubulin. Normalised differences (fold change) in Rad18-poly-ubiquitylation intensity between samples were analysed by densitometry and are depicted in red.

Figure 4 A consensus USP7 binding motif in Rad18 is important for its stability. **A** Purified GST-tagged fragments of Rad18 were mixed with purified Flag-tagged USP7 and GST-pulldowns were performed as described in Materials and Methods. A schematic of the Rad18 fragments utilized is depicted (right panel). **B** GST pull-downs were performed as in part 'A' but this time with a WT Rad18 fragment D or a mutant fragment D in which either S183 or S192/194 had been mutated to alanine (mutations denoted with X). The levels of co-precipitated USP7 were determined by Western Blotting. USP7 binding motifs identified in proteins known to interact with USP7 are shown. A comparison with two putative USP7 binding motifs identified in Rad18 is also shown. **C** 293FT cells were treated as in Figure 3A, except that cells were transfected with full length HA-tagged *Rad18* (WT) or a mutant HA-tagged *Rad18* where the serines S192 and 194 had been mutated to alanine and EGFP-

USP7. HA-tagged Rad18 was immunoprecipitated from cell extracts using anti-HA antibodies and the immuno-precipitated material was subjected to SDS-Page/Western blotting and the co-associated proteins detected with the indicated antibodies. **D** MRC5 cells were transfected with an empty vector (v) or a construct expressing either WT HA-tagged Rad18 or the S192/194A mutant HA-tagged Rad18. The cells were then incubated in media containing cycloheximide at a concentration of 60μg/ml for the indicated periods. Extracts from these cells were fractionated by SDS-Page and the levels of Rad18 determined by Western blotting. β-Actin was used as a loading control. **E** MRC5 cells were treated as in part 'D' with the exception that prior to DNA transfection endogenous USP7 was knocked down with siRNA. Quantification by densitometry of normalised HA-Rad18 protein levels in each sample is depicted in the graphs below Figures 4D and 4E, respectively. **F** MRC5 cells were transfected with a single Rad18 siRNA sequence for 48hrs and then with a siRNA-resistant *WT* or *S192/194A* HA-tagged *Rad18* construct only (left panel). 24hrs following transfection the cells were UV irradiated as indicated and 6hours later they were harvested. Extracts from the harvested cells were fractionated by SDS-Page and HA-Rad18 expression and PCNA monoubiquitylation was monitored by Western blotting. (left panel). These cells were additionally transfected with p*EGPF-Pol* η (right panel), fixed 6 hours after UV-irradiation and EGFP-Pol η localization was analyzed by fluorescence microscopy (right panel). At least 300 cells were analysed per condition.

Supplementary Figures

Supplementary Figure 1 siRNA mediated knockdown of USP7 does not affect cell cycle progression or the expression of Rad18. A HeLa cells were transfected

with the indicated siRNA sequences and 48 or 72 hours later the cells were fixed with ethanol, stained with PI and subjected to Flow cytometry analysis. **B** Hela cells were transfected with control, USP7 or Rad18 siRNA and 48 or 72 hours later the cells were harvested and cDNA generated from the extracted RNA. *Rad18* mRNA was quantified using quantitative PCR (qPCR) and is represented as a percentage expression relative to control siRNA transfected cells following normalisation to β-actin mRNA.

Supplementary Figure 2 USP7 deficient cells display reduced levels of hydroxyurea-induced PCNA mono-ubiquitylation. A MRC5 cells were transfected with control or USP7 siRNA and 48hrs following siRNA transfection they were exposed to 1mM HU for 24 hours. Extracts from these cells were subjected to SDS-Page and the levels of USP7, Rad18 and PCNA mono-ubiquitylation were determined.

Supplementary Figure 3 USP7 depletion does not alter Pol η protein levels. A MRC5 cells were transfected with control or USP7 siRNA, UV irradiated with 20J/m^2 and then harvested at the indicated times. The levels of both USP7 and DNA Pol η were monitored by Western blotting. **B** 293T cells were transfected with control or USP7 siRNA, 72 hours later were harvested and the levels of USP7, Rad18 and DNA Pol η were analysed by Western blotting. The asterisk denotes a non-specific band. **C** MRC5 (lane 1) or XP30RO (XP-Variant) (lane 2) and XP30RO-Pol η complemented cells (lane 3) were all harvested and the levels of Pol η, TopBP1 and β-Tubulin were monitored by Western blotting using the indicated antibodies. The asterisk denotes a non-specific band. **D** MRC5 cells were transfected as in A and 72

hrs later they were incubated in media containing cycloheximide at a concentration of (100µg/ml) for the indicated periods. The efficiency of USP7 knockdown and protein half-life rates in the presence of cycloheximide were analysed using the indicated antibodies. The asterisk denotes a non-specific band.

Supplementary Figure 4 USP7 depletion gives rise to a PRR defect comparable to loss of Rad18

HeLa cells transfected with control, USP7 or Rad18 targeted siRNA were pulse-labeled with ^{3}H-Thymidine, UV-irradiated, and then genomic DNA was extracted. ^{3}H-Thymidine was measured using scintillation counter on fractions obtained from differential sucrose sedimentation centrifugation of the gDNA. The inset graph represents an estimation of the average DNA molecular weight across the distribution normalized to the control siRNA.

Supplementary Figure 5 HLTF depletion does not affect the induction or the levels of PCNA mono-ubiquitylation following UV irradiation. A Hela cells were transfected with USP7 siRNA and 72 hours following transfections the levels of both USP7 and HLTF were analysed by Western blotting. The asterisk denotes a non-specific band. **B** MRC5 cells were transfected with control or HLTF specific siRNA, irradiated with 20J/m^2 of UV and then harvested at various times post-irradiation. The efficiency of HTLF knockdown, Rad18 levels and the ubiquitylation of PCNA were all determined by Western blotting.

Supplementary Figure 6 Rad18 is specifically de-ubiquitylated *in vitro* by USP7 but not USP25. *In vitro* ubiquitylation reactions using E1, Rad6, Rad18 and ubiquitin

were carried out as in Figure 3C. For the de-ubiquitylation assays, after the 3 hour ubiquitylation reaction, recombinant USP7 or USP25 was added to the mixture and the reactions were incubated for a further 2 hours at 37°C. The reactions were terminated by the addition of Laemli buffer and boiling. The proteins were detected using the indicated antibodies.

Figure 1

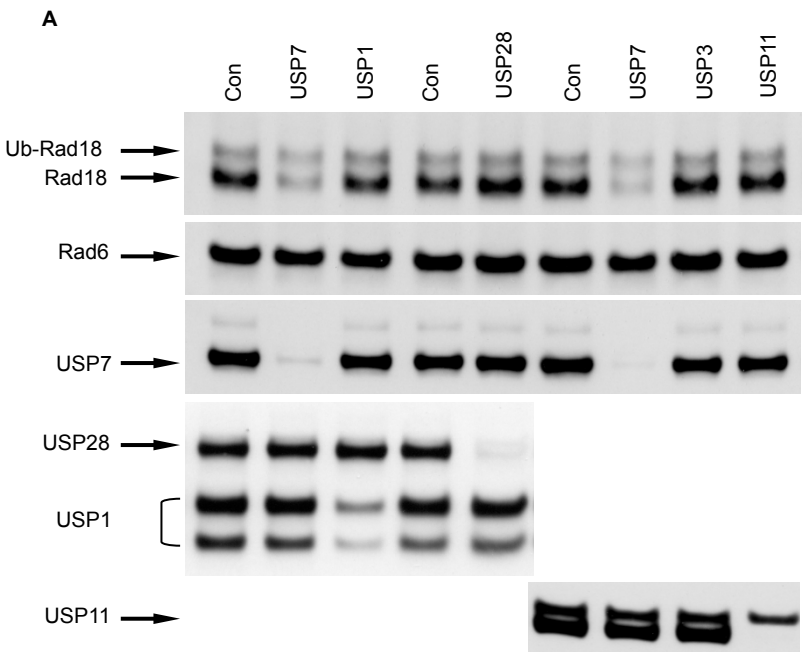
A
Con
USP7
USP1
Con
USP28
Con
USP7
USP3
USP11
Ub-Rad18
Rad18
Rad6
USP7
USP28
USP1
USP11

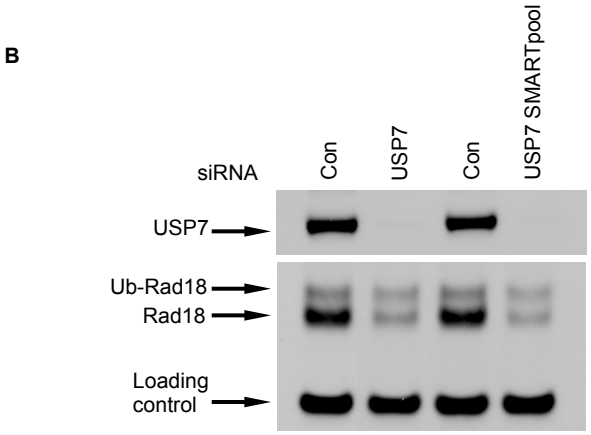
B
siRNA
Con
USP7
Con
USP7 SMARTpool
USP7
Ub-Rad18
Rad18
Loading
control

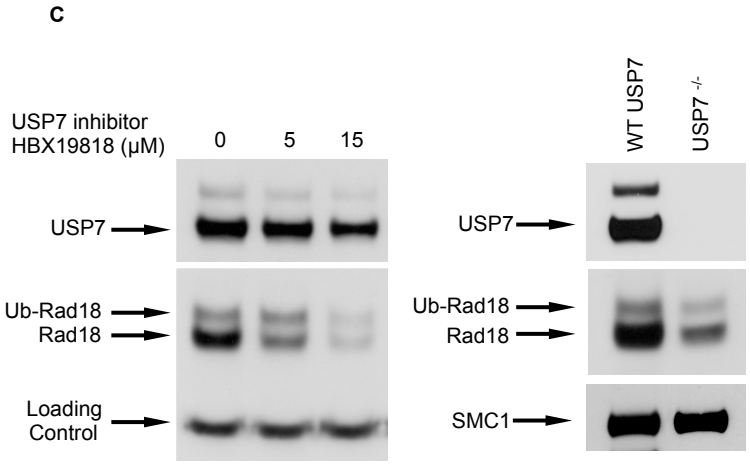
C
USP7 inhibitor
HBX19818 (μM)
0
5
15
USP7
Ub-Rad18
Rad18
Loading
Control
WT USP7
USP7 -/-
USP7
Ub-Rad18
Rad18
SMC1

Figure 1

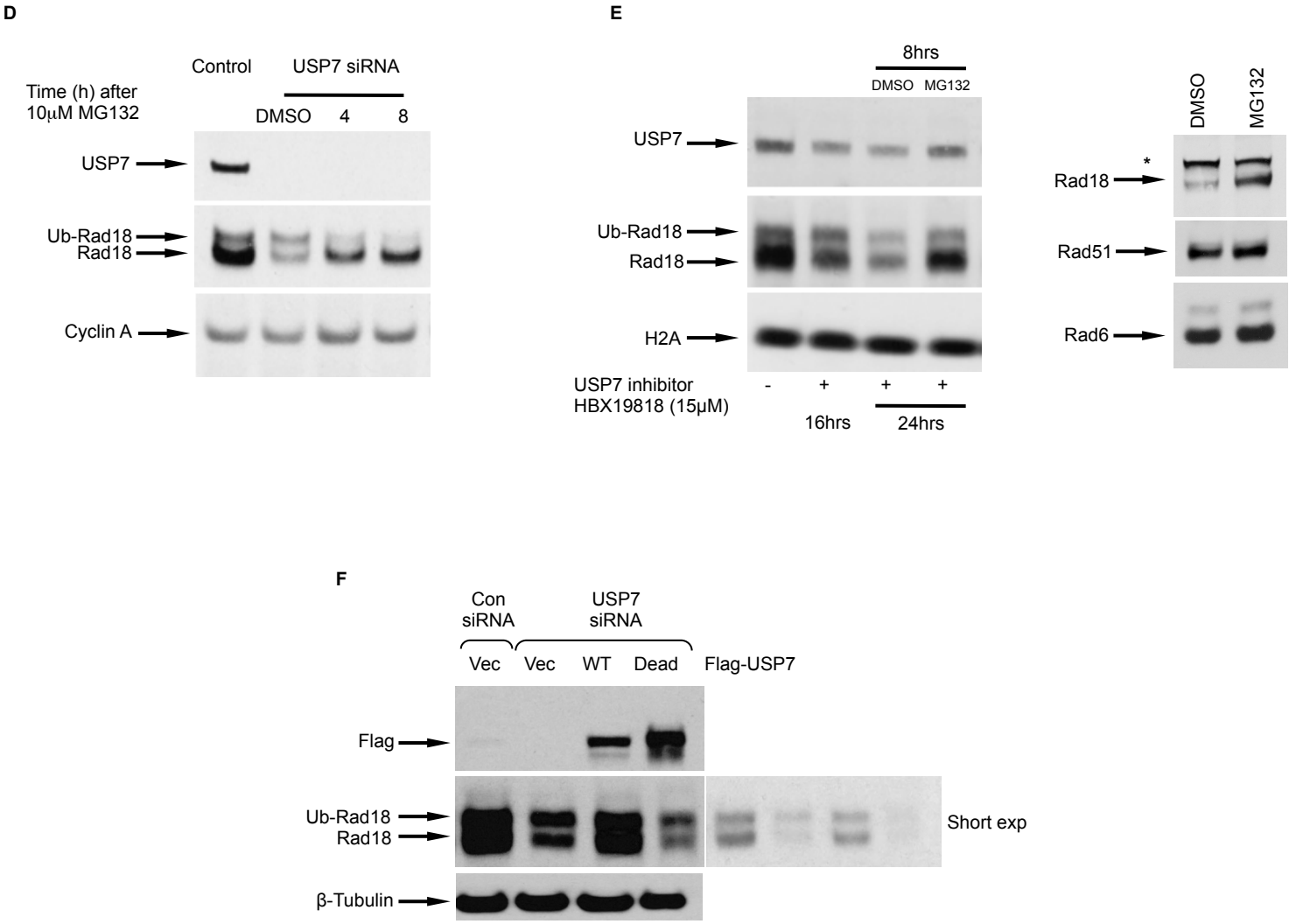
D
Control
USP7 siRNA
Time (h) after
10μM MG132
DMSO
4
8
USP7
Ub-Rad18
Rad18
Cyclin A
E
8hrs
DMSO
MG132
USP7
Ub-Rad18
Rad18
H2A
USP7 inhibitor
HBX19818 (15μM)
-
+
+
+
16hrs
24hrs
DMSO
MG132
*
Rad18
Rad51
Rad6
F
Con
siRNA
USP7
siRNA
Vec
Vec
WT
Dead
Flag-USP7
Flag
Ub-Rad18
Rad18
Short exp
β-Tubulin

Figure 2

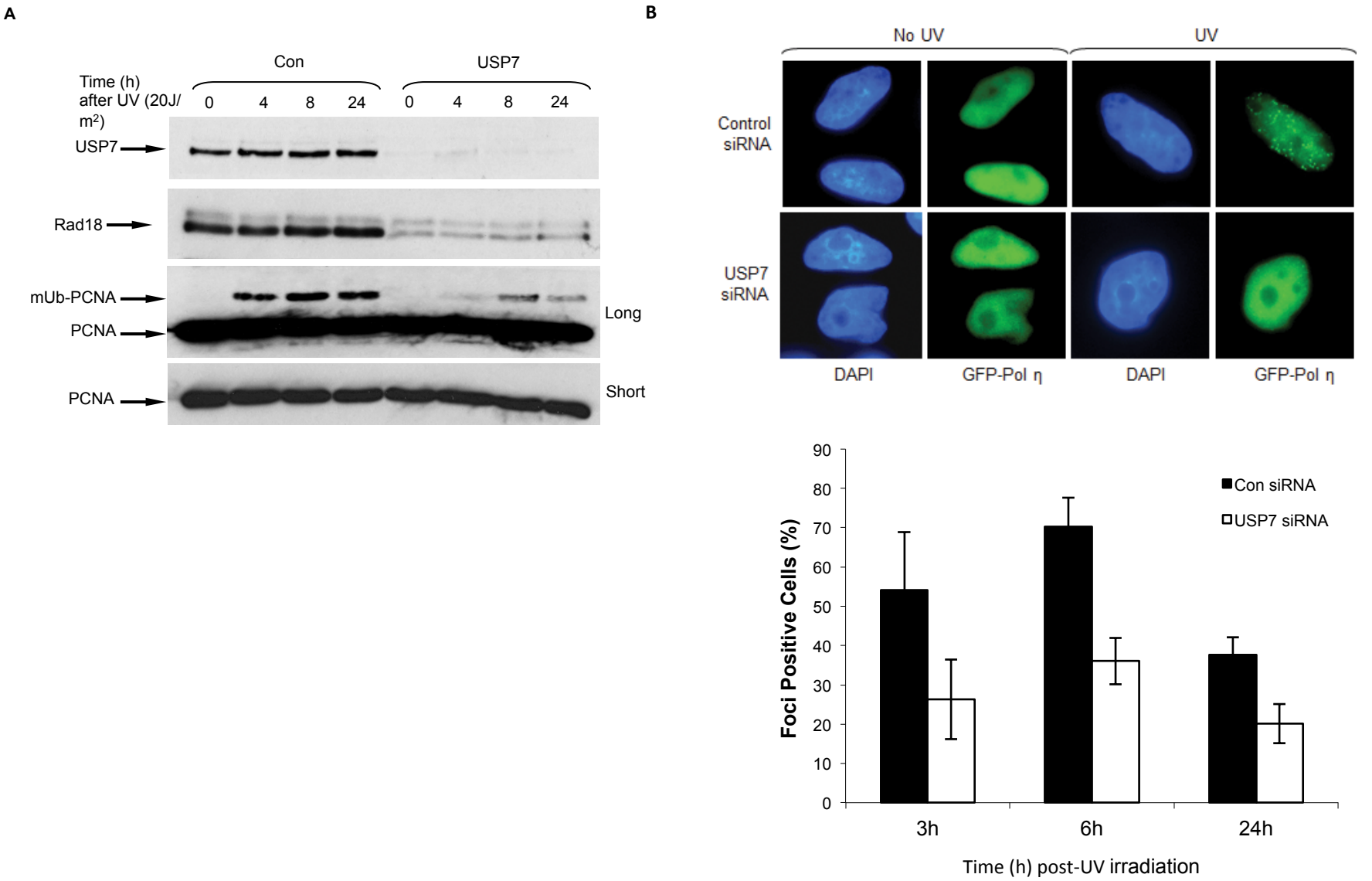
A
Con
USP7
Time (h) after UV (20J/m²)
0 4 8 24 0 4 8 24
USP7
Rad18
mUb-PCNA
PCNA
Long
PCNA
Short
B
No UV
UV
Control siRNA
USP7 siRNA
DAPI
GFP-Pol η
DAPI
GFP-Pol η
Foci Positive Cells (%)
90
80
70
60
50
40
30
20
10
0
Con siRNA
USP7 siRNA
3h
6h
24h
Time (h) post-UV irradiation

Figure 2

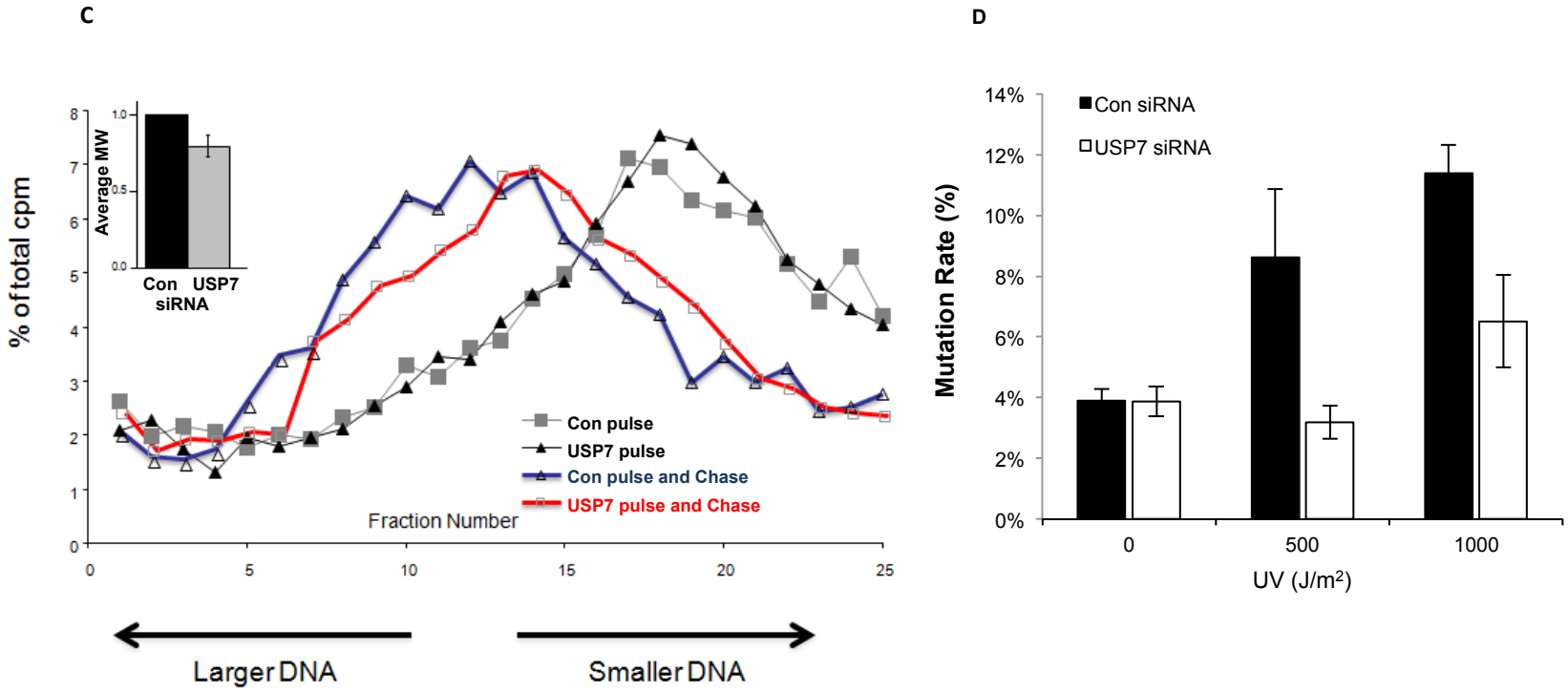
C
% of total cpm
Average MW
1.0
0.5
0.0
Con
USP7
siRNA
Con pulse
USP7 pulse
Con pulse and Chase
USP7 pulse and Chase
Fraction Number
Larger DNA
Smaller DNA
D
Mutation Rate (%)
Con siRNA
USP7 siRNA
14%
12%
10%
8%
6%
4%
2%
0%
0
500
1000
UV (J/m2)

Figure 2

E

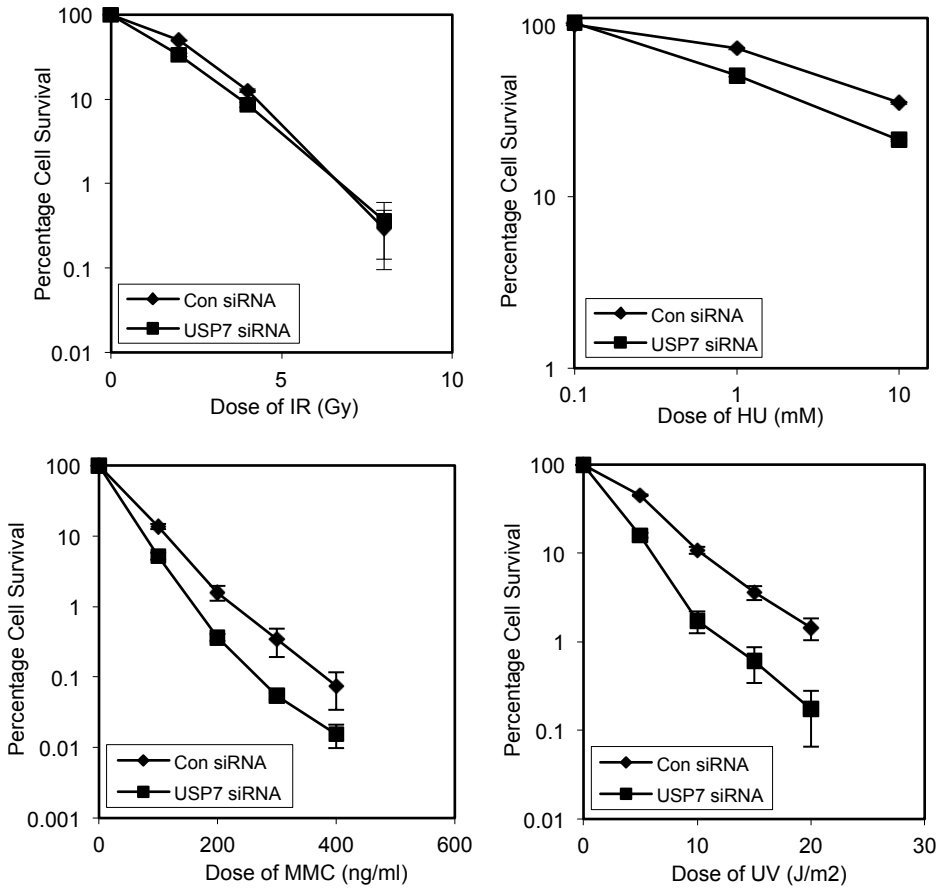
Percentage Cell Survival
Dose of IR (Gy)
Con siRNA
USP7 siRNA
Dose of HU (mM)
Dose of MMC (ng/ml)
Dose of UV (J/m2)

Figure 2

F

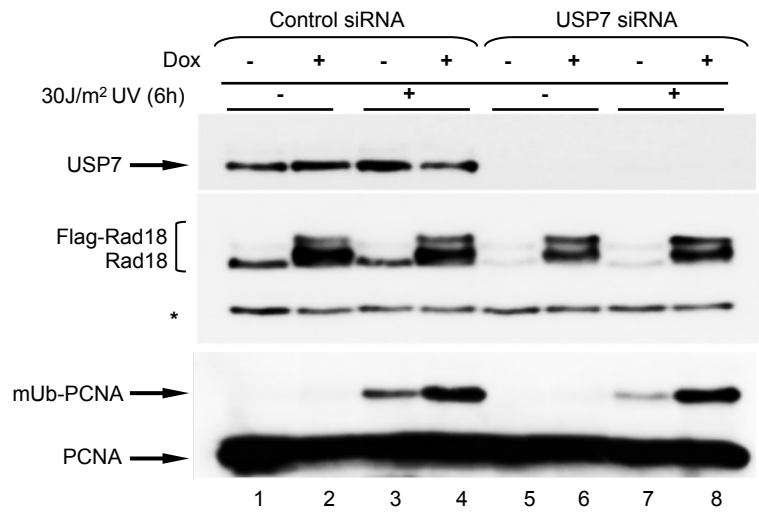
Control siRNA
USP7 siRNA
Dox
- + - + - + - +
30J/m2 UV (6h)
- + - +
USP7
Flag-Rad18
Rad18
*
mUb-PCNA
PCNA
1 2 3 4 5 6 7 8

Figure 3

A

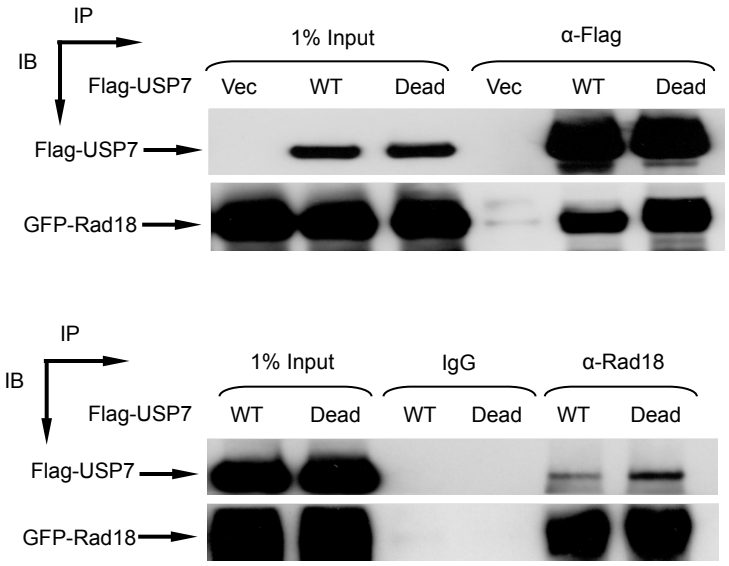
IP
IB
Flag-USP7
1% Input
α-Flag
Vec
WT
Dead
Vec
WT
Dead
Flag-USP7
GFP-Rad18
IP
IB
Flag-USP7
1% Input
IgG
α-Rad18
WT
Dead
WT
Dead
WT
Dead
Flag-USP7
GFP-Rad18

B

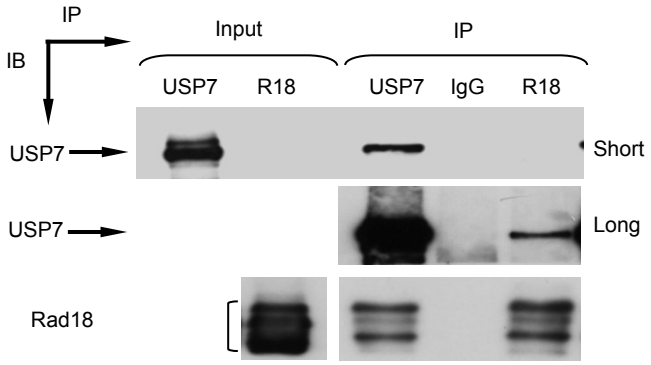
IP
IB
Input
IP
USP7
R18
USP7
IgG
R18
USP7
Short
USP7
Long
Rad18

Figure 3

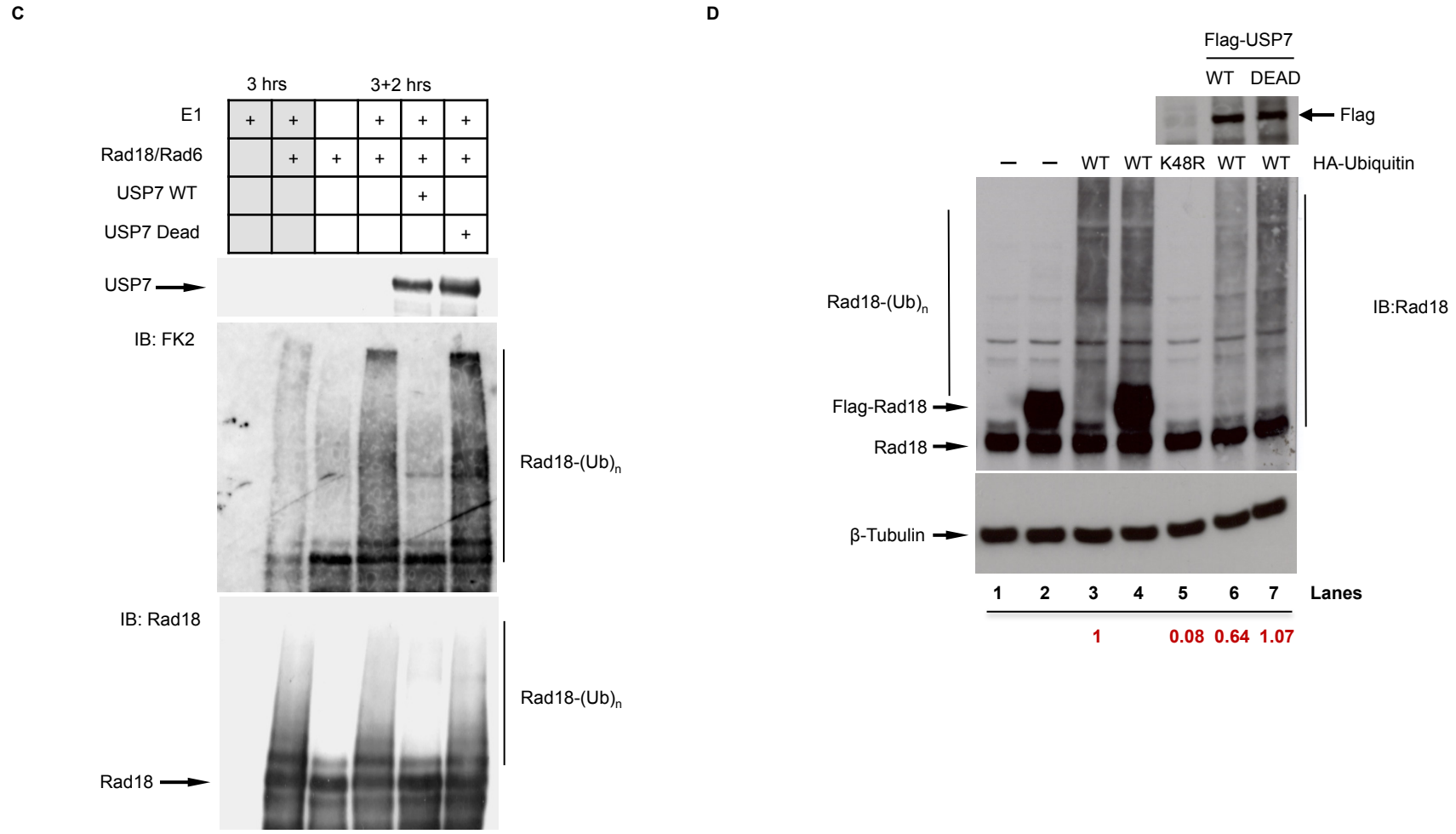
C
3 hrs
3+2 hrs
E1
Rad18/Rad6
USP7 WT
USP7 Dead
USP7
IB: FK2
Rad18-(Ub)n
IB: Rad18
Rad18-(Ub)n
Rad18
D
Flag-USP7
WT DEAD
Flag
— — WT WT K48R WT WT HA-Ubiquitin
Rad18-(Ub)n
IB:Rad18
Flag-Rad18
Rad18
β-Tubulin
1 2 3 4 5 6 7 Lanes
1 0.08 0.64 1.07

Figure 4

A

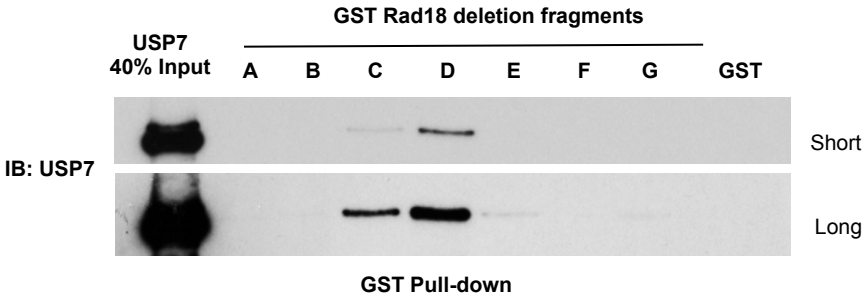
GST Rad18 deletion fragments
USP7
40% Input
A
B
C
D
E
F
G
GST
IB: USP7
Short
Long
GST Pull-down

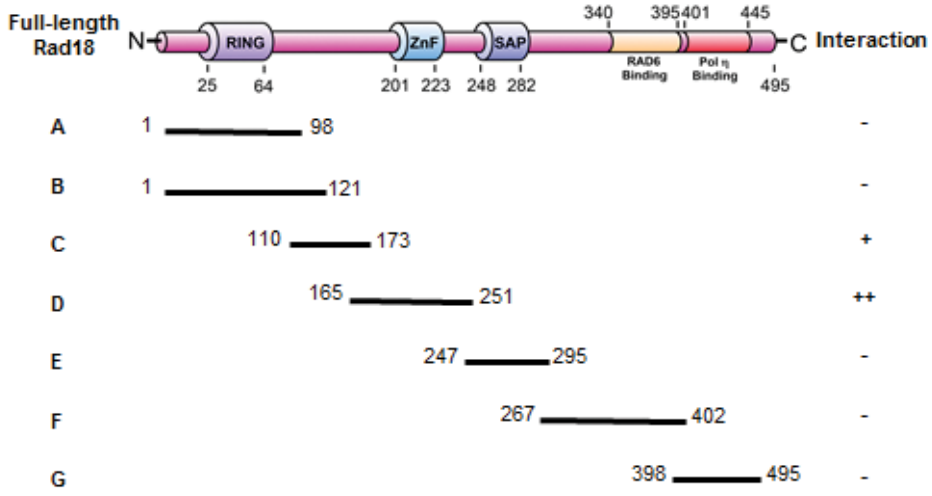
Full-length
Rad18
N
RING
ZnF
SAP
C
340
395
401
445
25
64
201
223
248
282
RAD6
Binding
Pol η
Binding
495
Interaction
A 1 98 -
B 1 121 -
C 110 173 +
D 165 251 ++
E 247 295 -
F 267 402 -
G 398 495 -

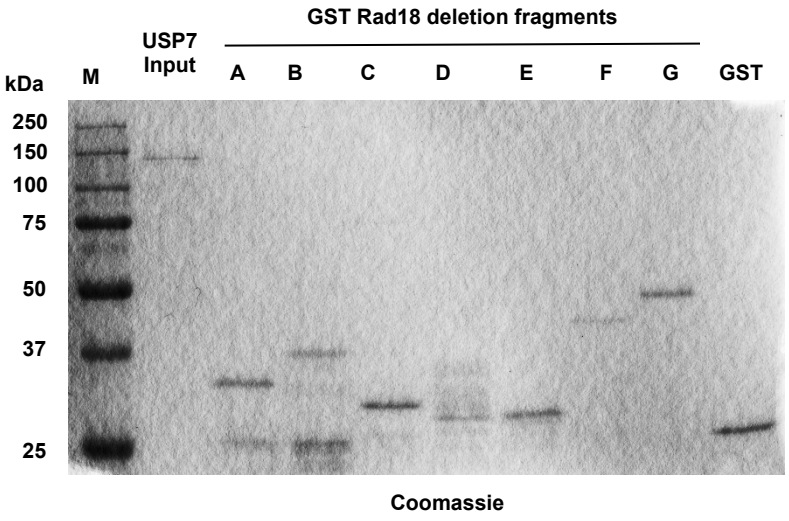
GST Rad18 deletion fragments
USP7
Input
kDa
M
A
B
C
D
E
F
G
GST
250
150
100
75
50
37
25
Coomassie

Figure 4

B

USP7 recognition Motif: **P/AxxS**

MDM2:	^{145}EKPS^{148} ^{147}PSSS^{150} ^{157}PSTS^{160} ^{397}PSTS^{400}
MDMX:	^{8}AQCS^{11} and ^{398}AHSS^{401}
EBNA1:	^{445}PGEGPS^{450}
p53:	^{359}PGGS^{362} ^{364}AHSS^{367}
Rad18:	^{179}**PDPS**^{183}EAKRPEP ^{190}**PSTS**^{194}

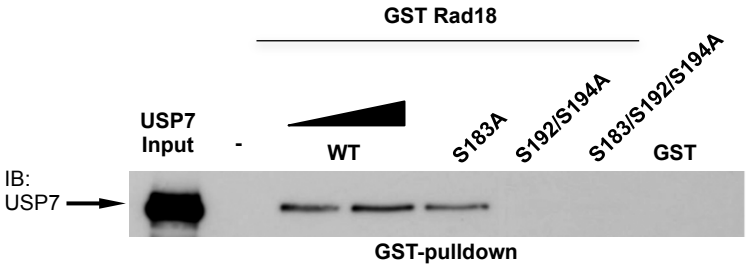

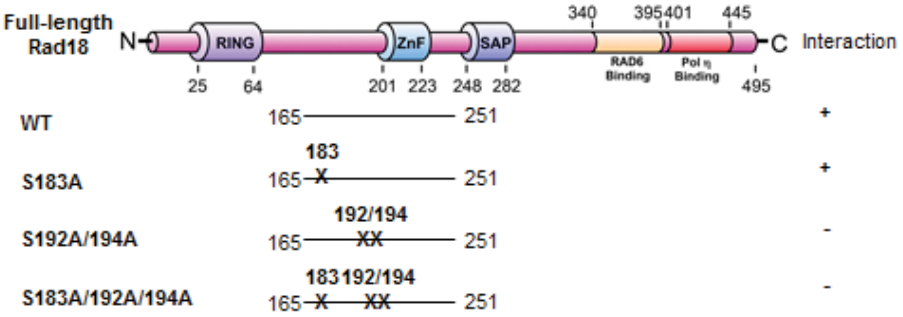

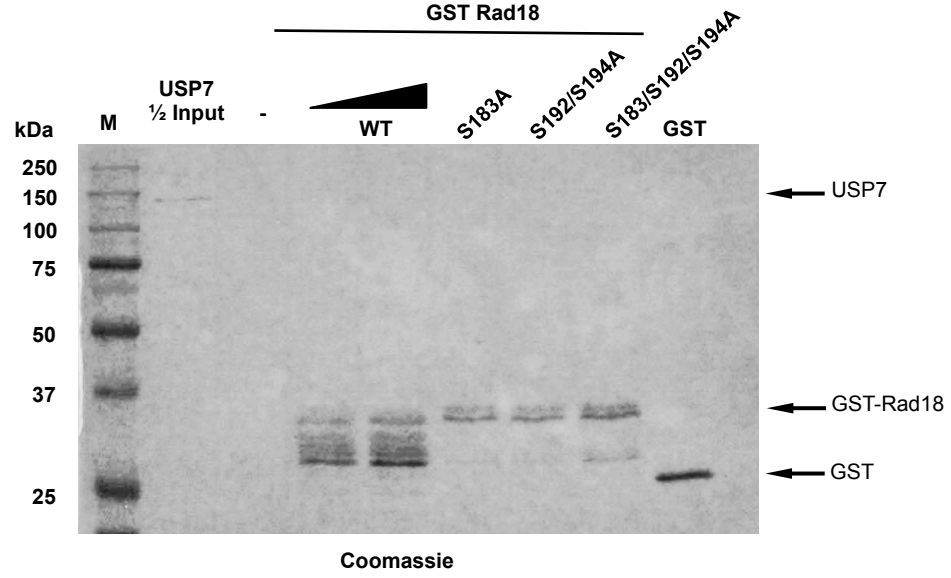

Figure 4

C

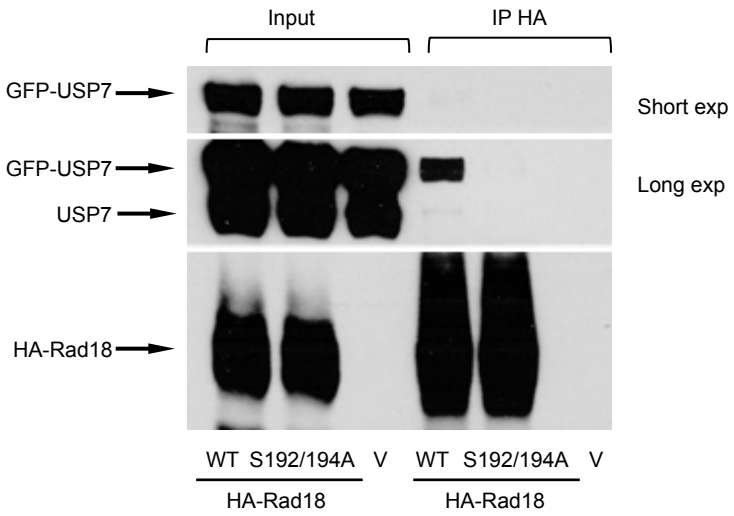
Input
IP HA
GFP-USP7
GFP-USP7
USP7
HA-Rad18
Short exp
Long exp
WT S192/194A V
HA-Rad18
WT S192/194A V
HA-Rad18

Figure 4

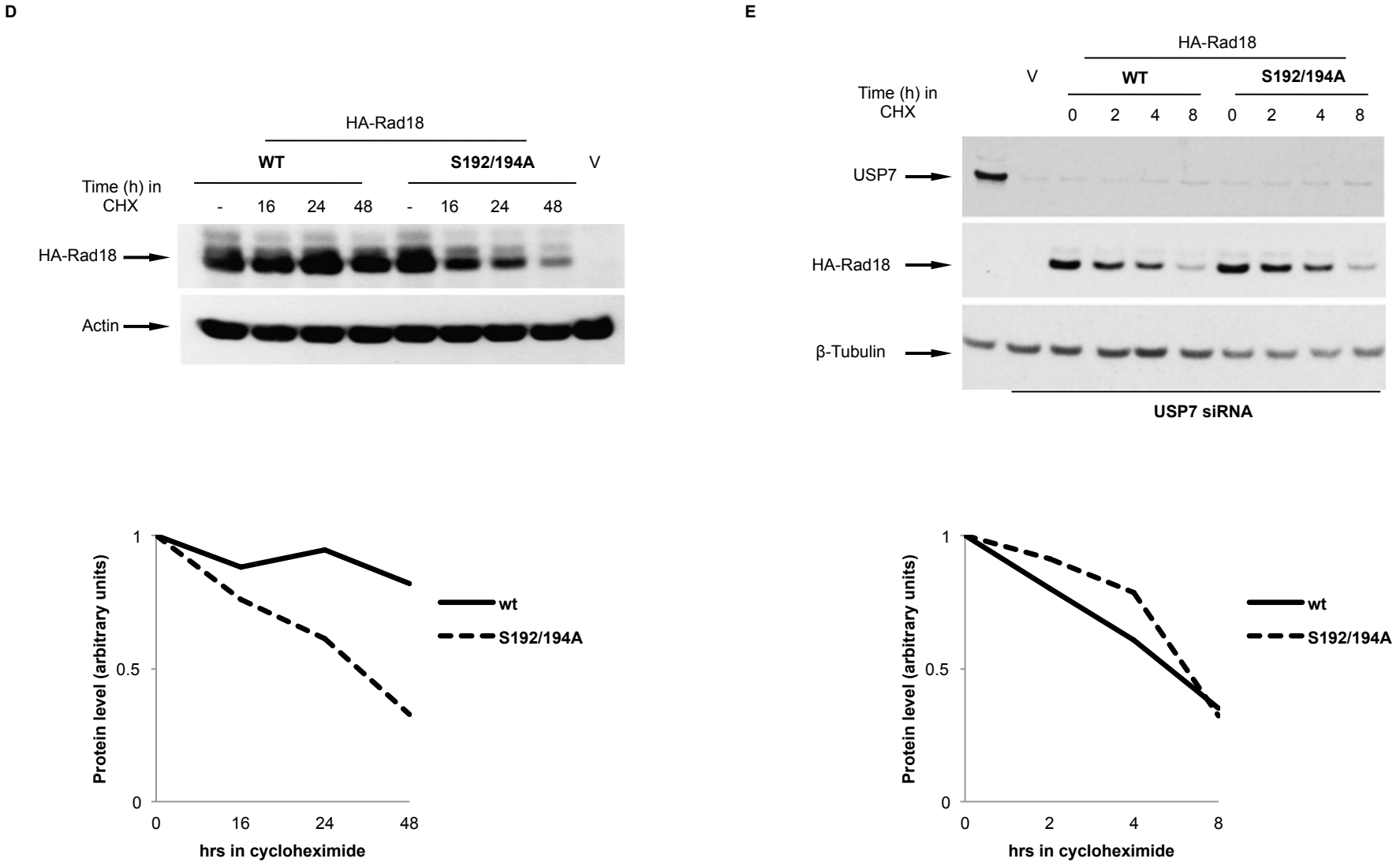
D
HA-Rad18
WT
S192/194A
V
Time (h) in CHX
- 16 24 48 - 16 24 48
HA-Rad18
Actin
E
HA-Rad18
V
WT
S192/194A
Time (h) in CHX
0 2 4 8 0 2 4 8
USP7
HA-Rad18
β-Tubulin
USP7 siRNA
Protein level (arbitrary units)
1
0.5
0
0 16 24 48
hrs in cycloheximide
wt
S192/194A
Protein level (arbitrary units)
1
0.5
0
0 2 4 8
hrs in cycloheximide
wt
S192/194A

Figure 4

F

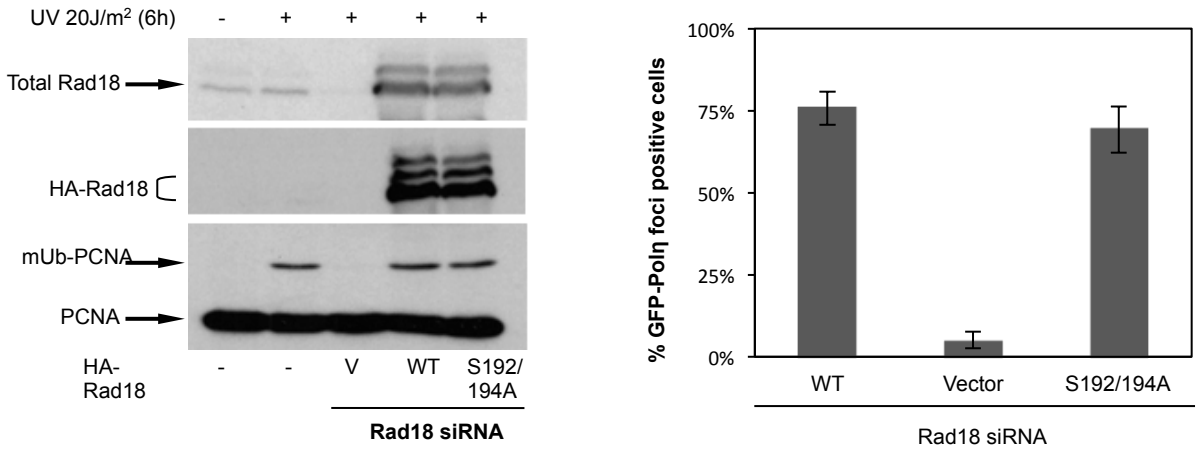
UV 20J/m2 (6h)
-
+
+
+
+
Total Rad18
HA-Rad18
mUb-PCNA
PCNA
HA-Rad18
-
-
V
WT
S192/194A
Rad18 siRNA

% GFP-Polη foci positive cells
100%
75%
50%
25%
0%
WT
Vector
S192/194A
Rad18 siRNA

Supplementary Figure 1

A

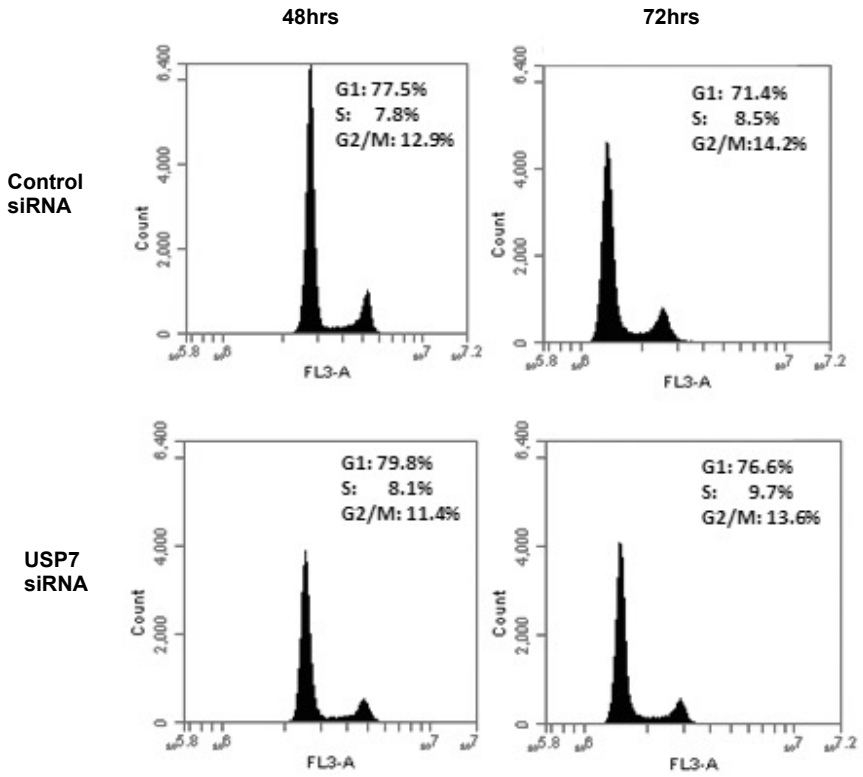

B

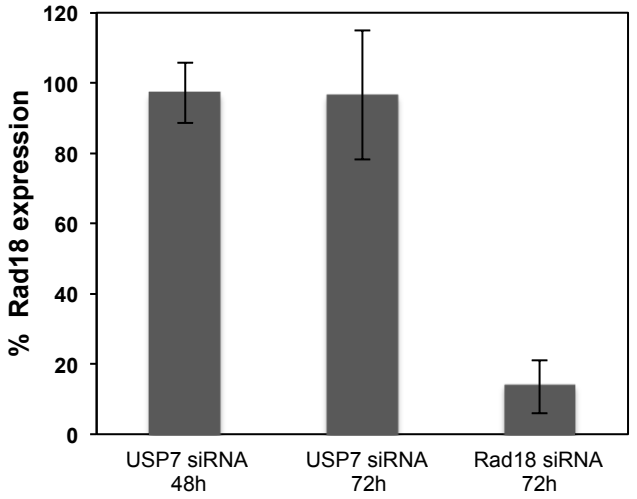

Supplementary Figure 2

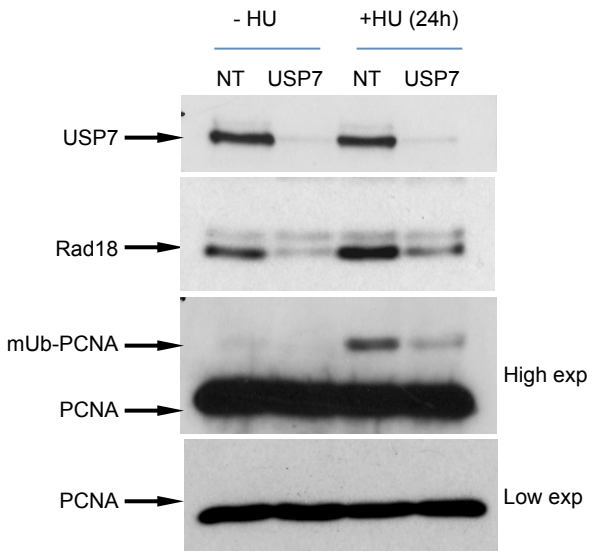

Supplementary Figure 3

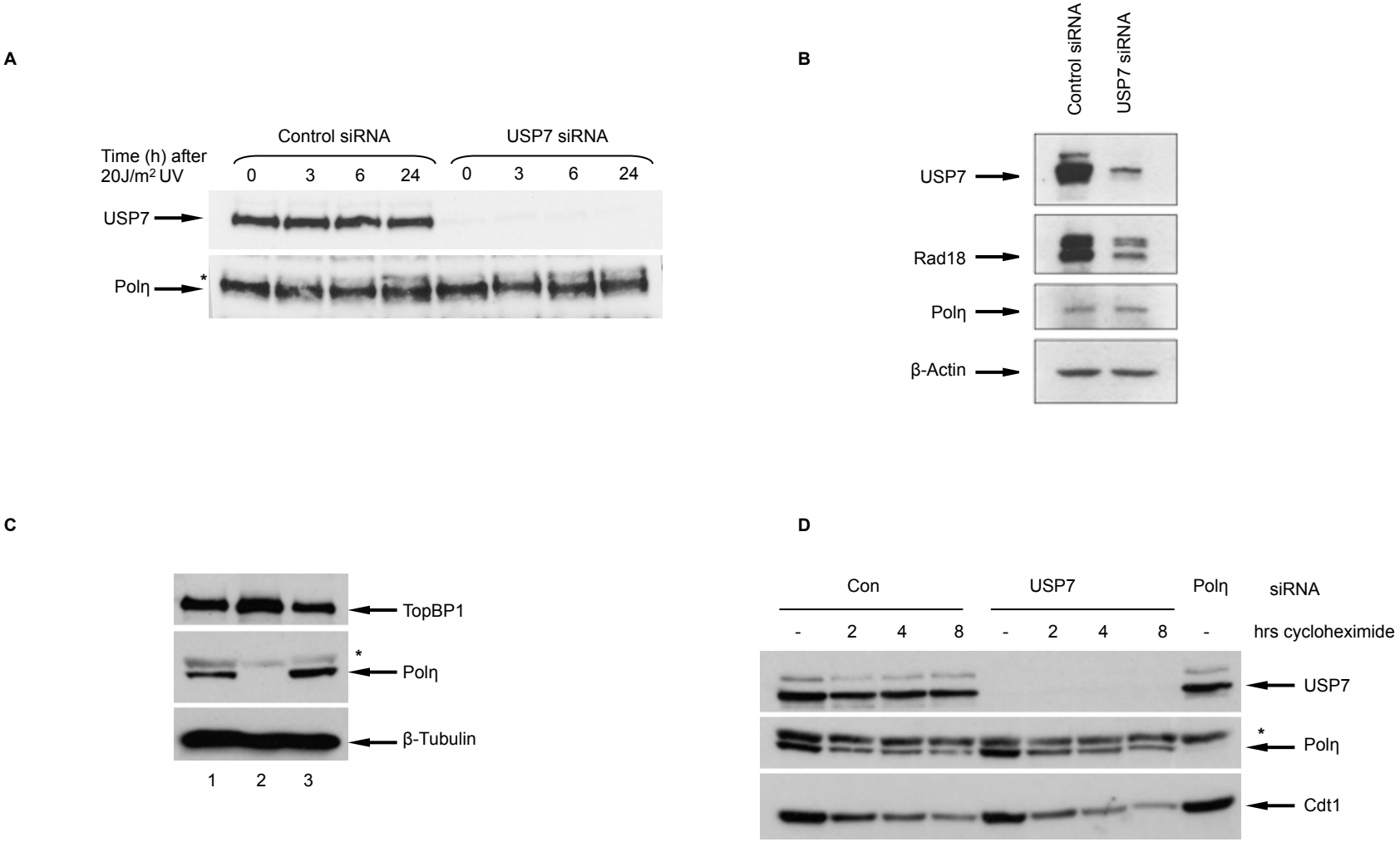

Supplementary Figure 4

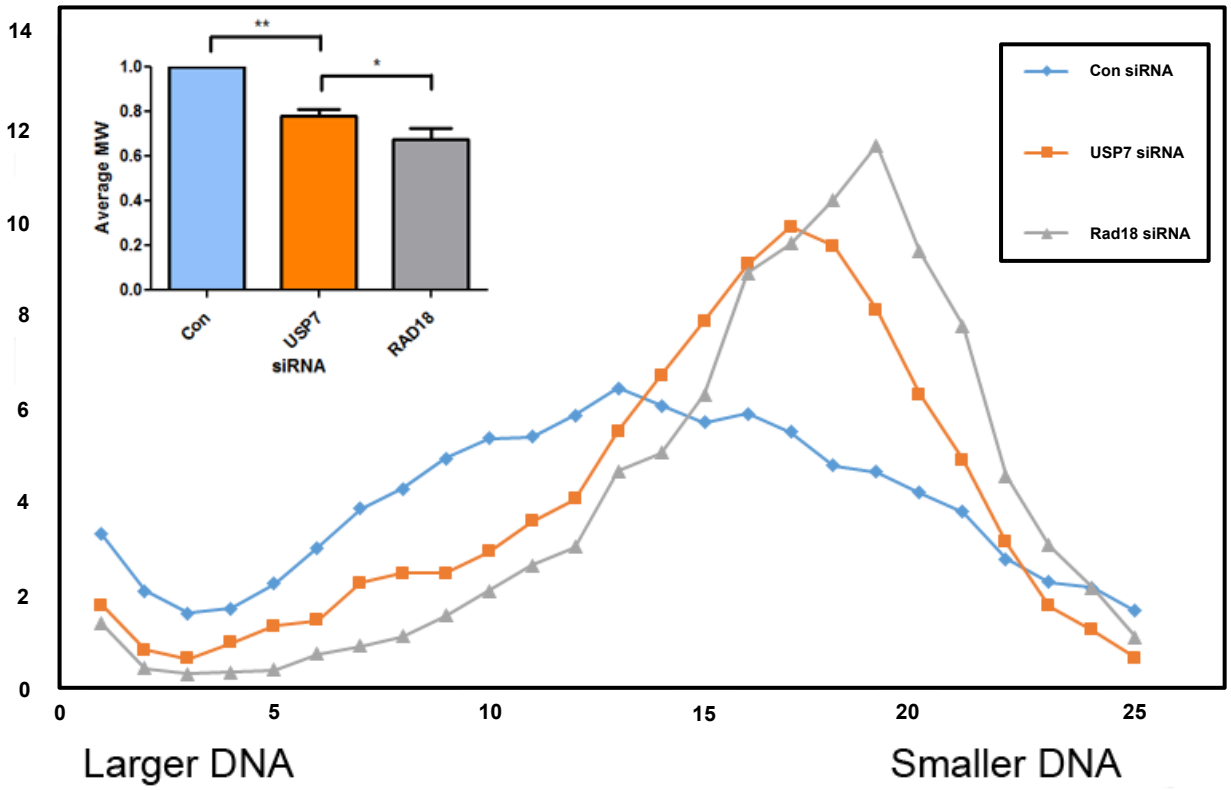

Supplementary Figure 5

A

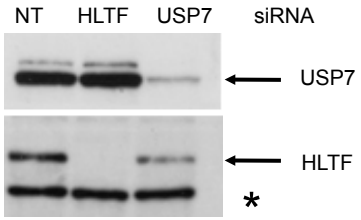

B

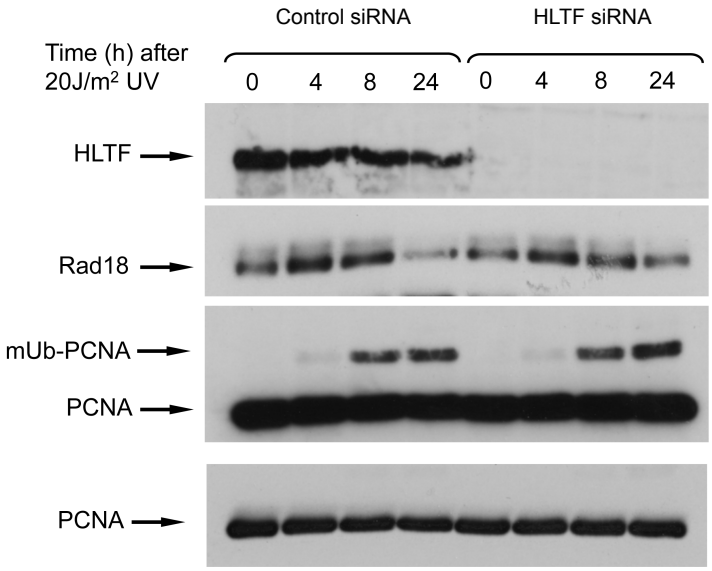

Supplementary Figure 6